Development and Prospects of Continental-Scale Resistivity Surveying for Orogenic Processes and Resource Controls

Philip Wannamaker[1]

[1]University of Utah, Energy & Geoscience Institute

November 23, 2022

Abstract

At regional scales, electrical resistivity illuminates Earth processes involving fluid evolution and transport, temperature contrasts, and fault characteristics and behavior. It also clarifies continental terrane assembly and event sequencing through electronic mineral markers. Magnetotellurics (MT) is sensitive over such scales, but faces high property contrasts, small signals, 3-D complexity, discontinuous fields, and ill-posed inversion. So-called wideband (˜0.003 – 500 s wave period) MT recording constrains crustal structure, and high fidelity through its central dead band is routinely achieved now via distant remote referencing, continuous streaming, and outlier removal. To resolve across the upper mantle, long period data must be of high quality through 10,000 s. Electronics modifications now permit good quality MT data over polar ice-covered regions, and non plane wave outliers appear largely avoidable. Regularized 3D non-linear inversion using simulation equations that recognize a spatially discontinuous electric field has become common practice and lends essential credibility to interpretations. However, resistivity model non-uniqueness is seldom tested enough, and assuming isotropic resistivity can lead to artifacts. Fluids interpreted to cause low resistivity in ductile deep crust should be at lithostatic pressures and have compositions compatible with ambient temperature and metamorphic grade. Vertical current channeling enhances resolution of large-scale fault zones connecting deep and shallow structures. Stabilized terranes can exhibit strong, quasi-linear conductors marking belts of graphite or sulfides deposited in sediment-starved foredeeps or rift margin basins, with a particular concentration in the Proterozoic corresponding to atmospheric oxygenation events. An exciting recent avenue is estimating H2O content of nominally anhydrous minerals (NAMs) in the upper mantle, which strongly affects electrical conductivity but not seismic velocity. The large bandwidth of MT data affords a broad-scale, unified view of Earth processes from mantle level sources through crustal storage and evolution to near-surface deposition. Support has been from U.S. Dept of Energy contract DE-0006732 and National Science Foundation grant OPP-1443532, and numerous prior.

Development and Prospects of Continental-Scale Resistivity Surveying for Orogenic Processes and Resource Controls

Philip E. Wannamaker, University of Utah/EGI,
423 Wakara Way, Ste 300, Salt Lake City, USA

U.S. National Science Foundation, U.S. Department of Energy

Source Fields for the Magnetotelluric Method

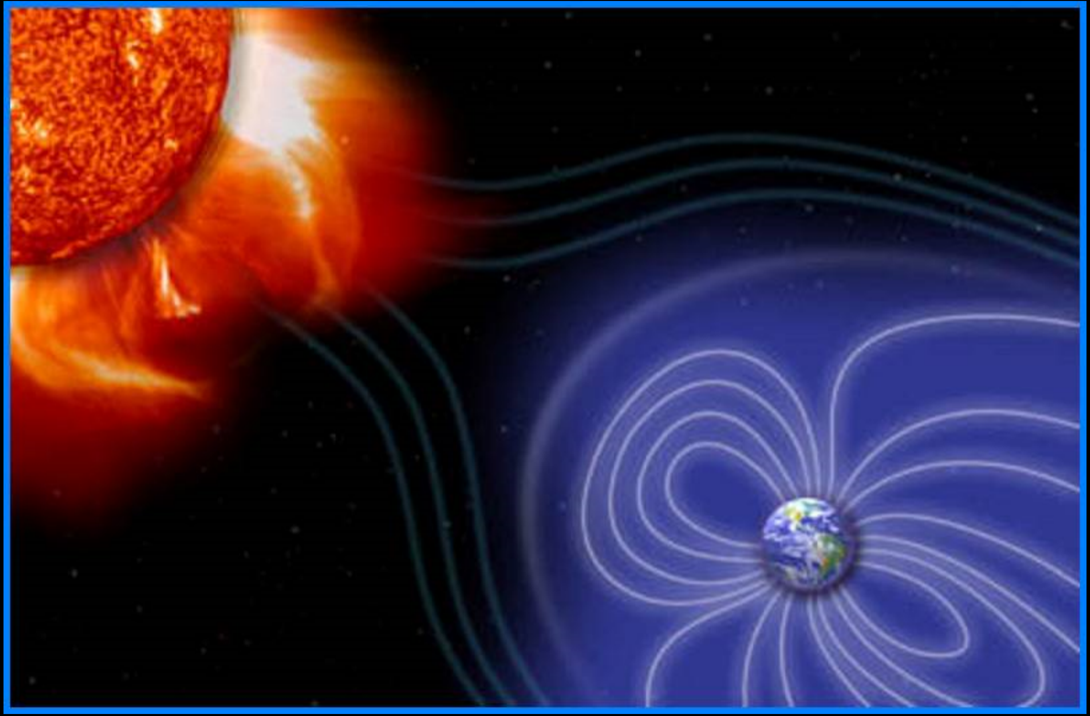

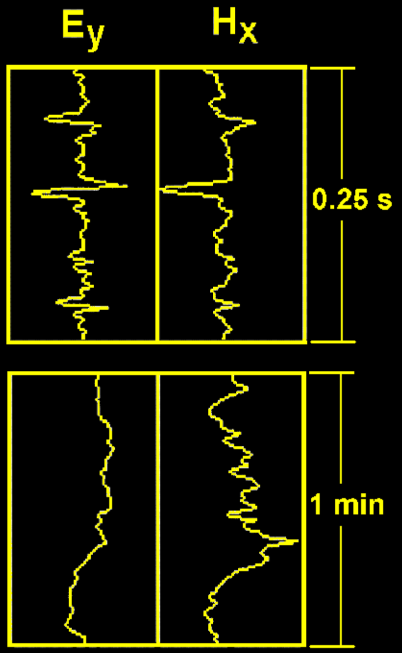

Regional and Global Lightning Activity for f > 1 Hz
Solar Wind-Magnetospheric Interactions for f < 1 Hz

Outline

<u>Incl. Historical Perspectives</u>

-MT Concepts Dev at MIT (T. Madden)

Tensor relation, Current Channeling, Staggered Grid 3D Modeling

Vertical current channeling insights into crustal rheology and geothermal systems, Current 3D inversion platforms

-Concepts Dev at UT Austin (F. Bostick)

Spectral Estimation, Cascade Decimation, Electromagnetic Array Profiling

Coherency sorting, Ultra-remote referencing

-Aqueous phase controls in lower crust and upper mantle

-MT surveying in polar regimes

Subduction/Backarc Extension and Continental Growth

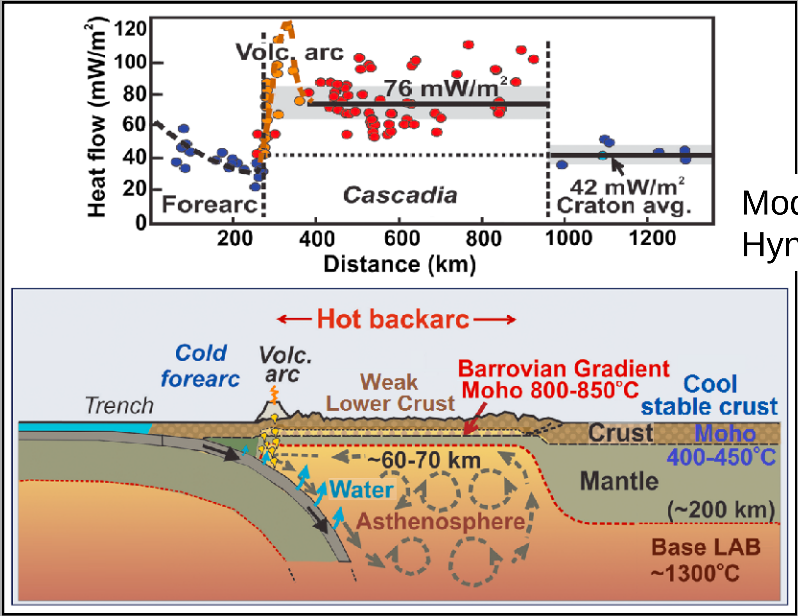

Modified from Hyndman (2018)

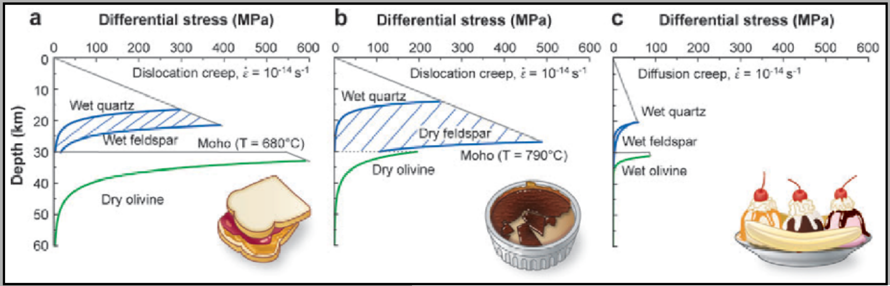

Burgmann and Dresen (2008)

$$H_2 = \alpha_{21}E_1 + \alpha_{22}E_2$$
$$H_1 = \alpha_{11}E_1 + \alpha_{12}E_2$$

Cantwell (1960, MIT)

Recognition of need for tensor relation

Wight et al (1977, UTA)

Cascade decimation and RT FT

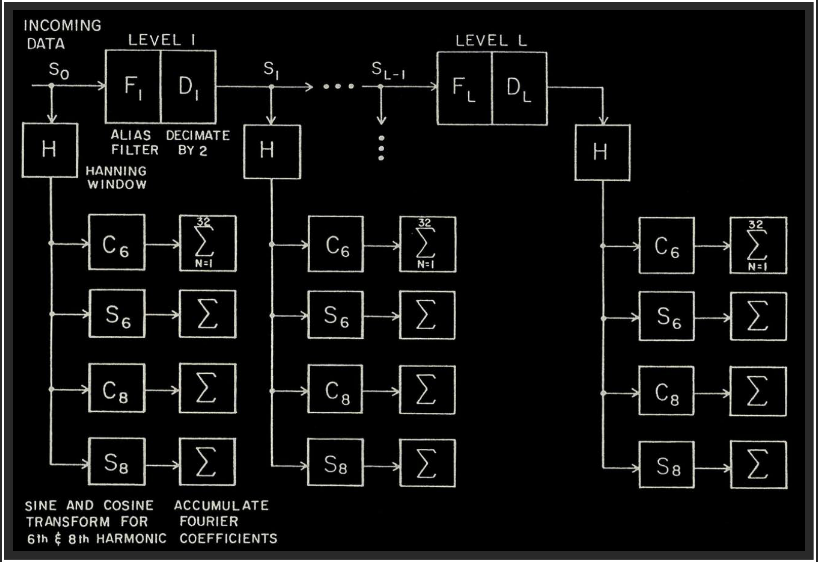

$$\begin{pmatrix} \mathrm{I} \\ \mathrm{II} \end{pmatrix} \qquad \begin{pmatrix} \mathrm{I} \\ \mathrm{II} \end{pmatrix} \qquad \begin{pmatrix} \mathrm{I} \\ \mathrm{II} \end{pmatrix}$$
$$\Phi_{h_1h_1}(\theta) = Y_{11}(\theta)\Phi_{h_1e_1}(\theta) + Y_{12}(\theta)\Phi_{h_1e_2}(\theta)$$
$$\begin{pmatrix} \mathrm{I} \\ \mathrm{II} \end{pmatrix} \qquad \begin{pmatrix} \mathrm{I} \\ \mathrm{II} \end{pmatrix} \qquad \begin{pmatrix} \mathrm{I} \\ \mathrm{II} \end{pmatrix}$$
$$\Phi_{h_2h_2}(\theta) = Y_{21}(\theta)\Phi_{h_2e_1}(\theta) + Y_{22}(\theta)\Phi_{h_2e_2}(\theta)$$

$$E_j(\theta) = \beta_{jk}E_k(0) \qquad [\beta_{ik}] = \begin{bmatrix} \cos\theta & \sin\theta \\ -\sin\theta & \cos\theta \end{bmatrix}$$
$$H_i(\theta) = \beta_{ik}H_k(0),$$

Bostick and Smith (1962, UTA)

Impedance elements from spectral cross powers

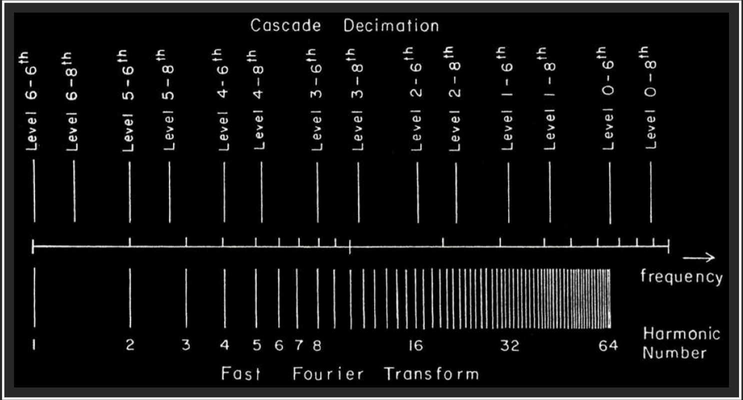

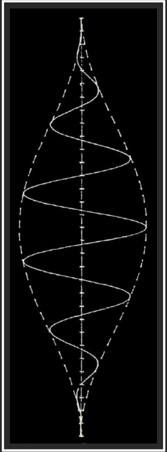

Cascade vs FFT log frequency spacing

$$Z_{xy} = \frac{(H_xH_x^*)(E_xH_y^*) - (E_xH_x^*)(H_xH_y^*)}{(H_xH_x^*)(H_yH_y^*) - (H_yH_x^*)(H_xH_y^*)}$$

Sims et al (1971)

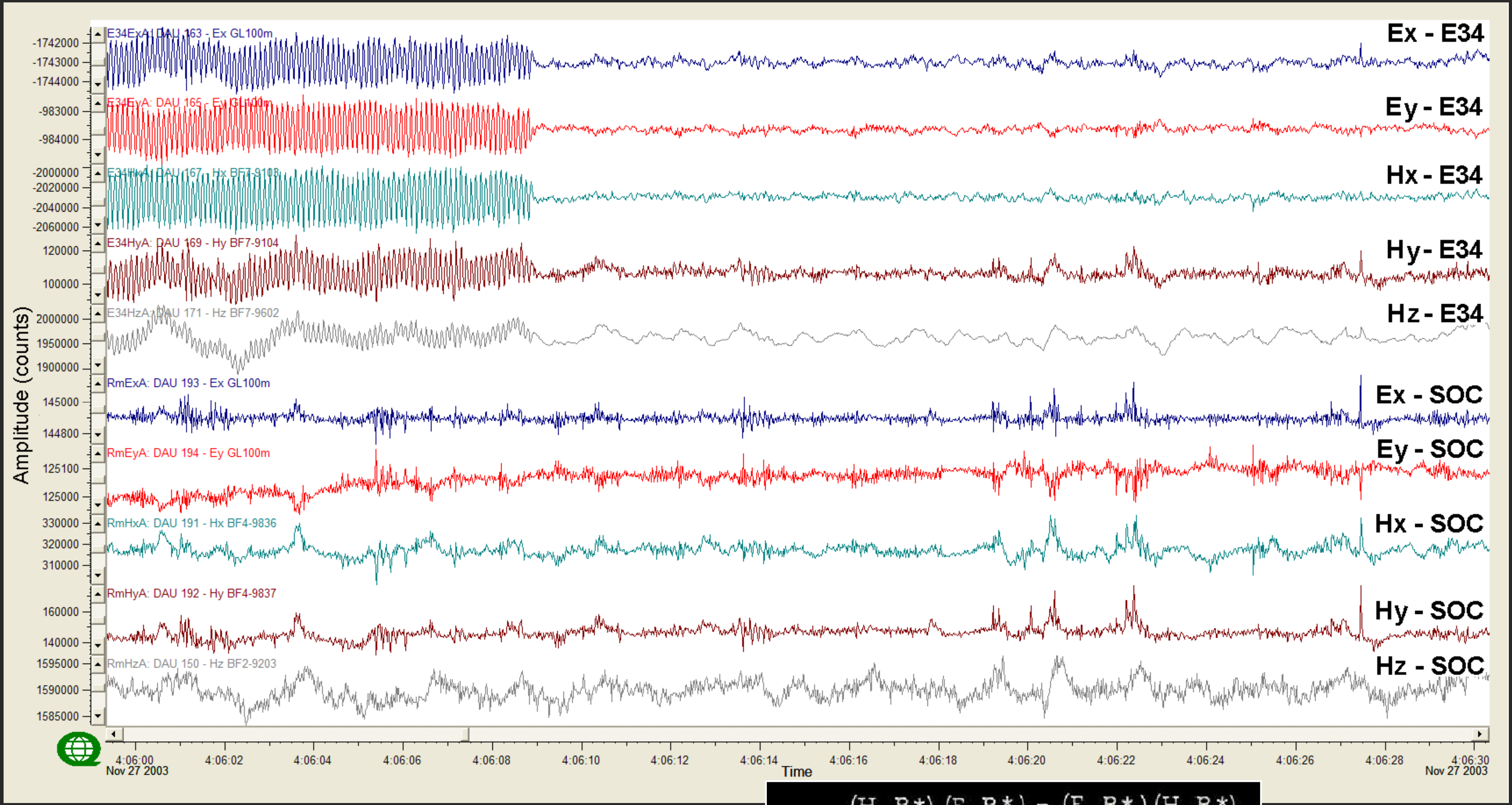

Local (noisy) vs Remote MT time series

Coso Geothermal Field (Wannamaker et al, 2004)

$$Z_{xy} = \frac{(H_x R_x^*)(E_x R_y^*) - (E_x R_x^*)(H_x R_y^*)}{(H_x R_x^*)(H_y R_y^*) - (H_y R_x^*)(H_x R_y^*)}$$

Clarke, Gamble, Goubau (1978)

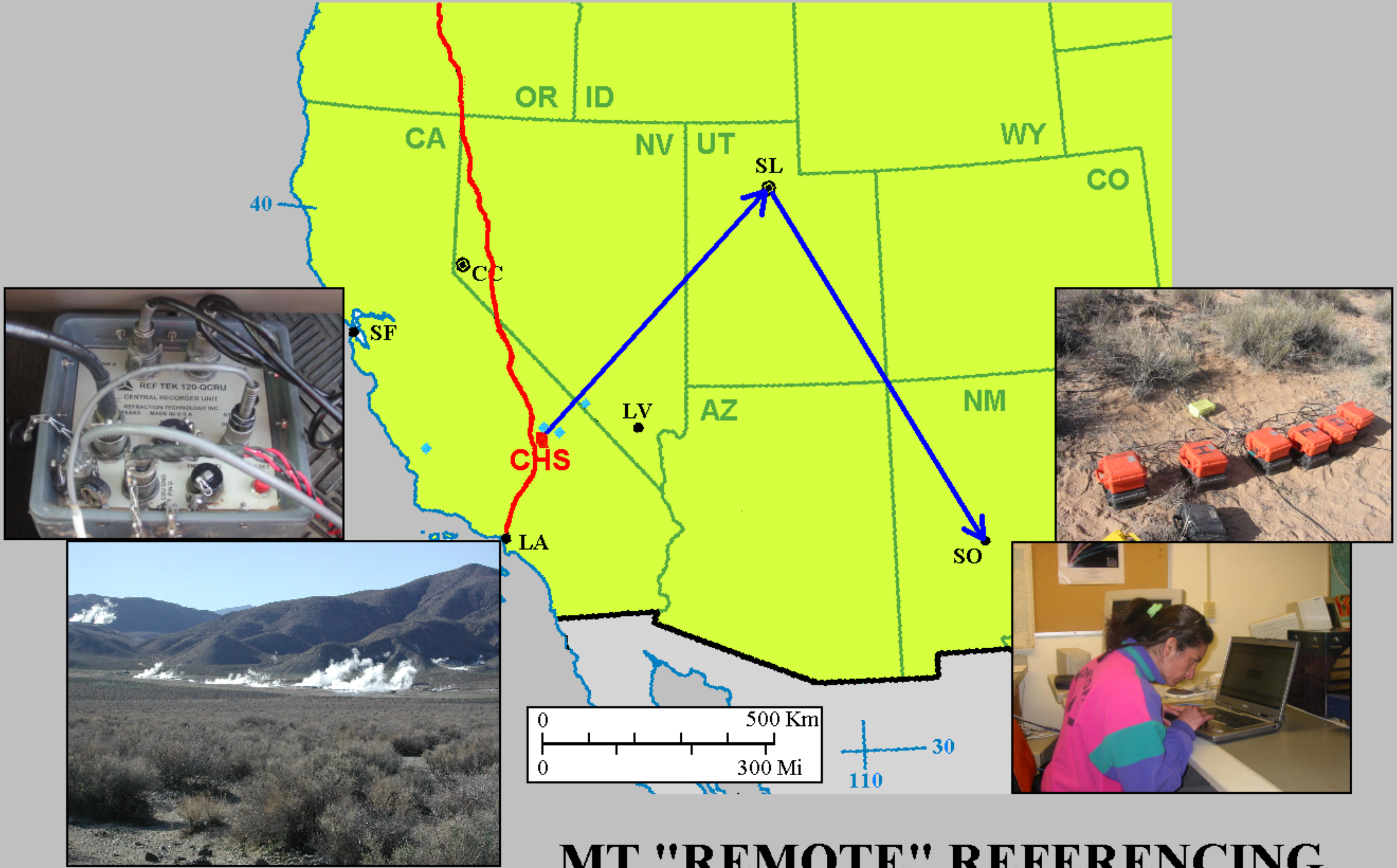

MT "REMOTE" REFERENCING

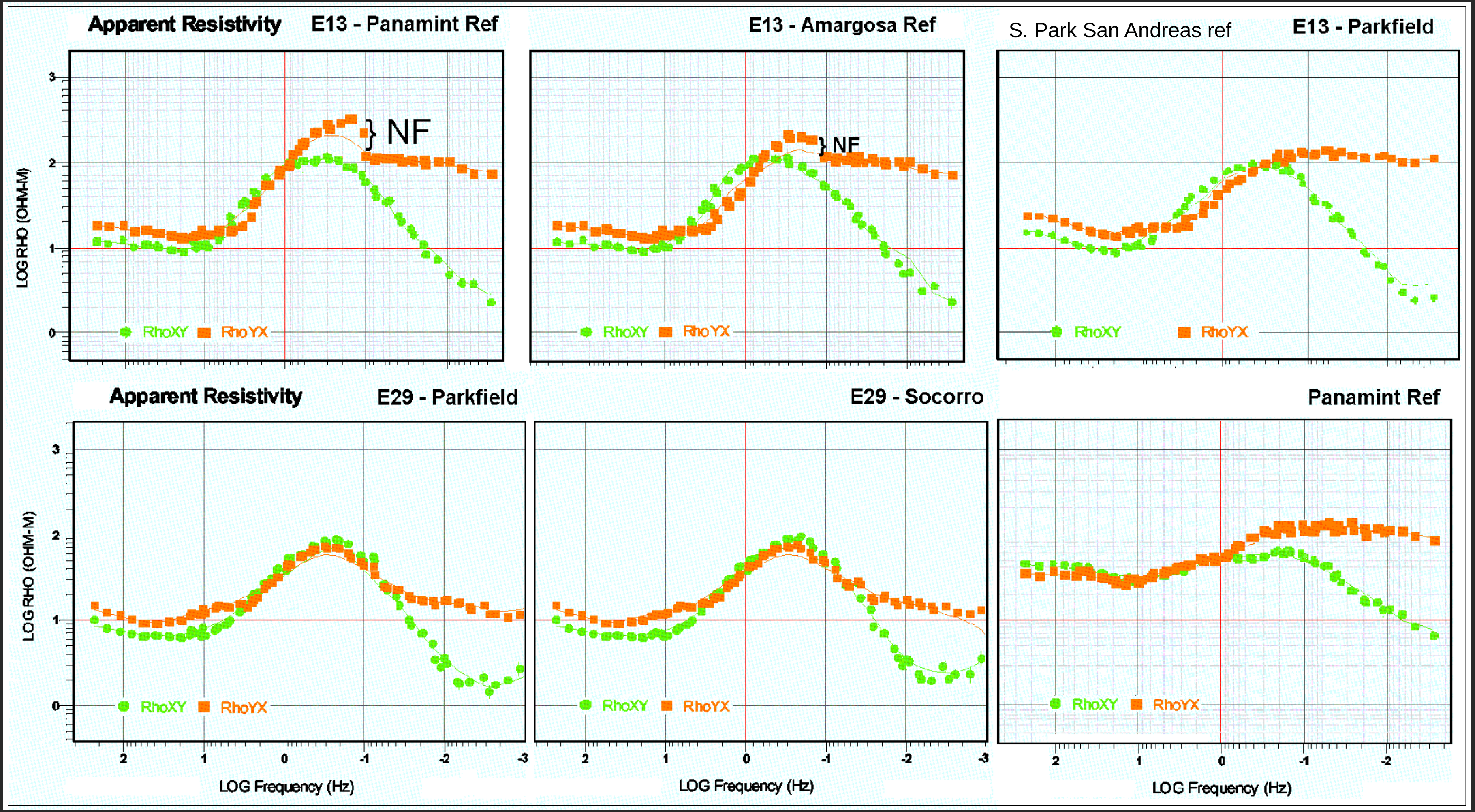

DC intertie near-field effect exceeds 150 km. Reference must be completely outside its field span even if plane wave by that point.

Swift (1967, MIT)

- -Assumed tensor relation from start
- -Elliptical traces in complex plane
- -Spectral analysis from time segments
- -Specified TE, TM modes

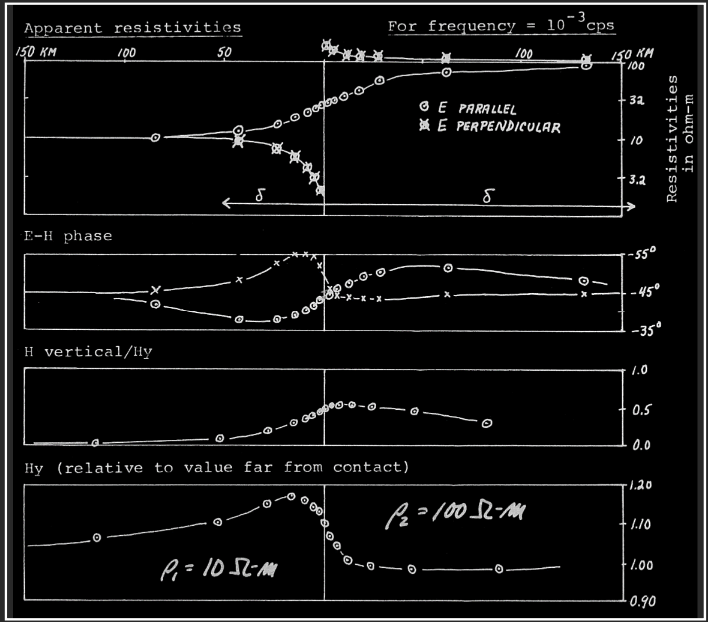

- -Collected 7 tensor sites in AZ and NM using ~50 km telephone lines; T = ~1000 s to ~1 da
- -2D forward modeling using FD code
- -Deeper upper mantle 10-30 ohm-m
- *-Noted that "TE" response inside truncated graben could be depressed*

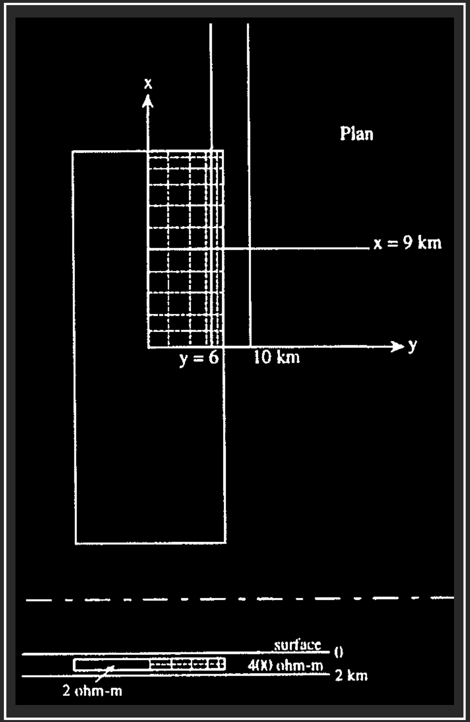

Wannamaker, Hohmann and Ward (1980, 1984); Ledo (2005)

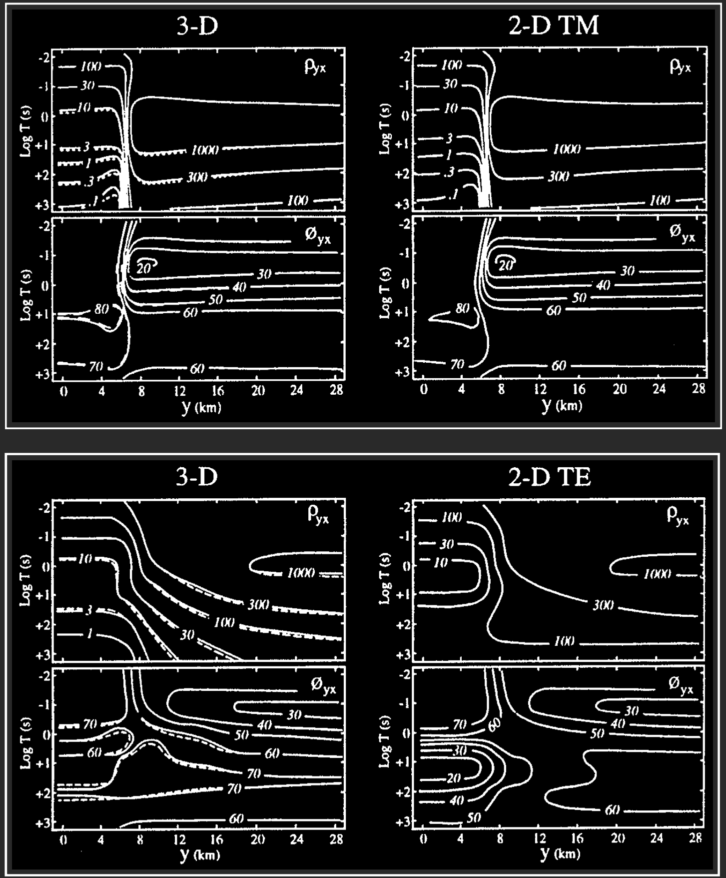

Similarity of 3D Zyx and 2D TM for simple bodies, incl. off-center
Disagreement of 3D Zxy and 2D TE due to boundary charges
More complex bodies increasingly 3D

Swift (1967, MIT)

- -Assumed tensor relation from start
- -Elliptical traces in complex plane
- -Spectral analysis from time segments
- -Specified TE, TM modes

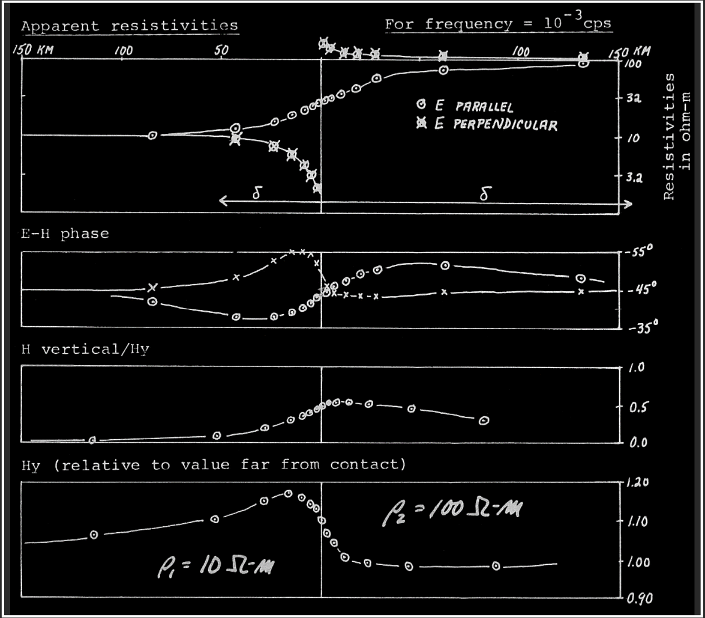

- -Collected 7 tensor sites in AZ and NM using ~50 km telephone lines; T = ~1000 s to ~1 da
- -2D forward modeling using FD code
- -Deeper upper mantle 10-30 ohm-m
- *-Noted that "TE" response inside truncated graben could be depressed*

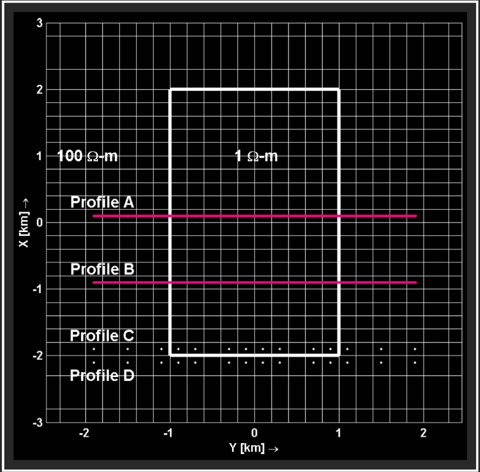

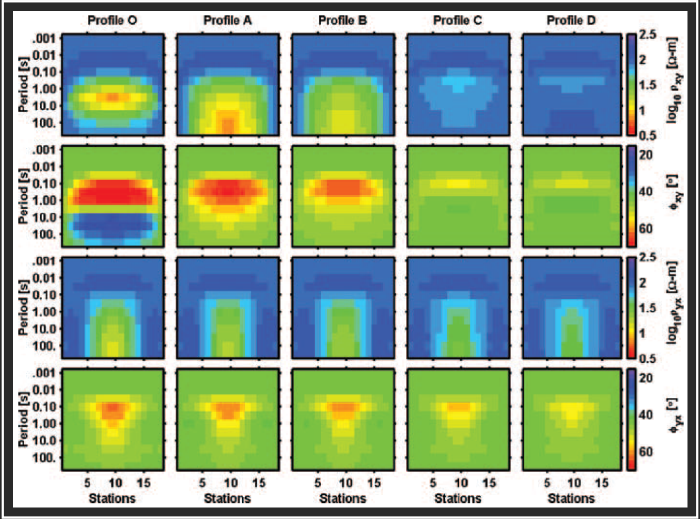

Siripunvaraporn et al, (2005)

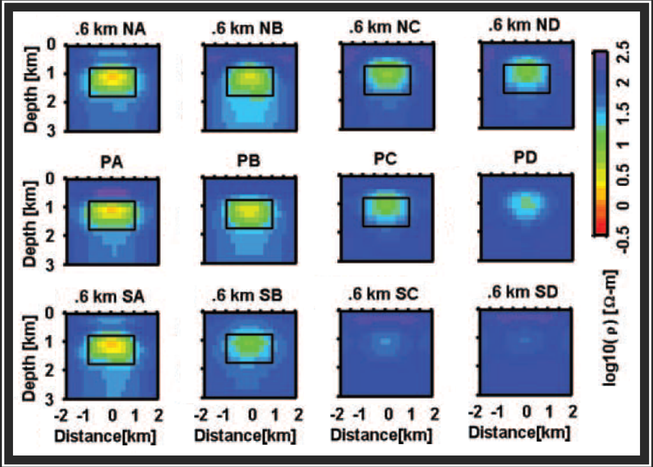

3D Profile Inversion Effective

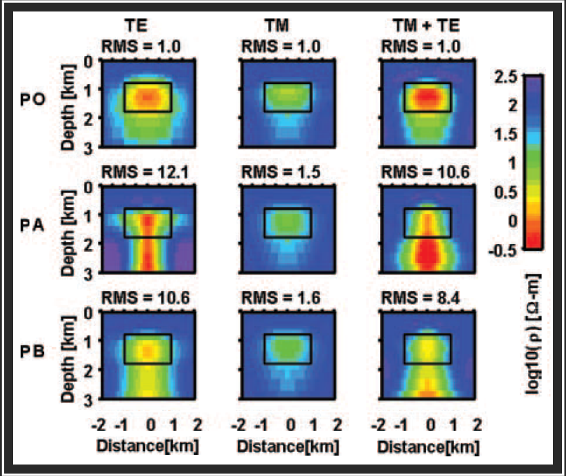

2D "TE" Inversion Distorted

Electromagnetic Simulation and Inversion With Conformal Receiver Surfaces (Topography)

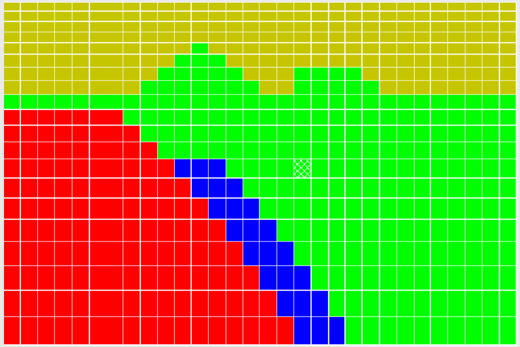

Finite Difference Topo Model

Graphics after Art Raiche

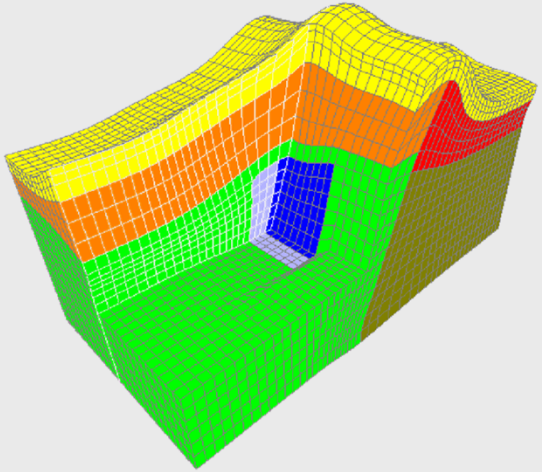

Finite Element Cutout View

$$\oint H \cdot dl = \iint \sigma E \cdot ds$$
$$\oint E \cdot dl = \iint \mu\omega H \cdot ds$$

e.g.,
$$(E_{xt} - E_{xb})/\Delta z - (E_{zr} - E_{zl})/\Delta x = i\omega\mu H_{yc}$$

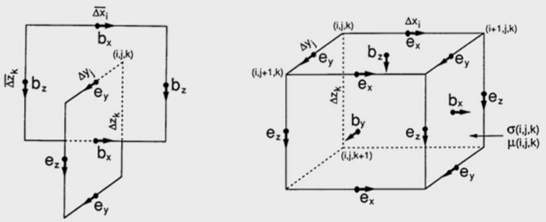

FD: Madden and Mackie (1989) resurrected Yee (1966) staggered grid. Numerous followers.

$$\nabla \times E = -i\omega\mu H \qquad \nabla \times H = \hat{\sigma} E$$
$$\nabla \times \frac{1}{\mu}\nabla \times E - i\omega\mu\hat{\sigma} E = J^{imp}$$
$$E = \sum_{i=1}^{n_e} x_i N_i \qquad H = \frac{-\nabla \times E}{i\omega}$$

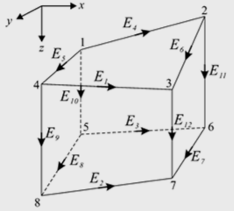

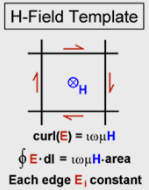

FE: E-field discontinuity treated with edge elements. Unambiguous placement of sharp interfaces.

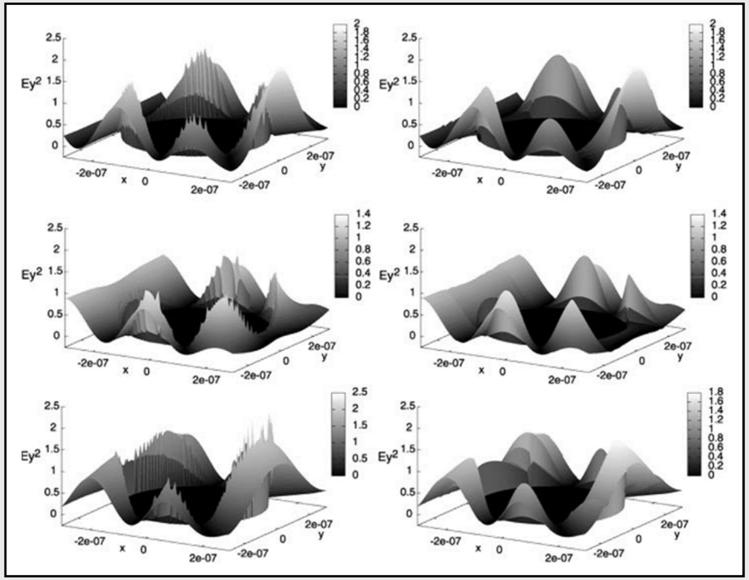

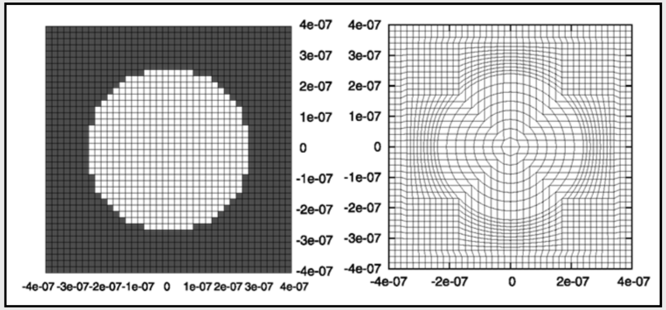

Scattered E Power
Liu et al., 2009

Torres-Verdin and Bostick (1992, UTA)
-Sampling challenge in natural environs
-E-field anomalies zero-mean, incl. 3D

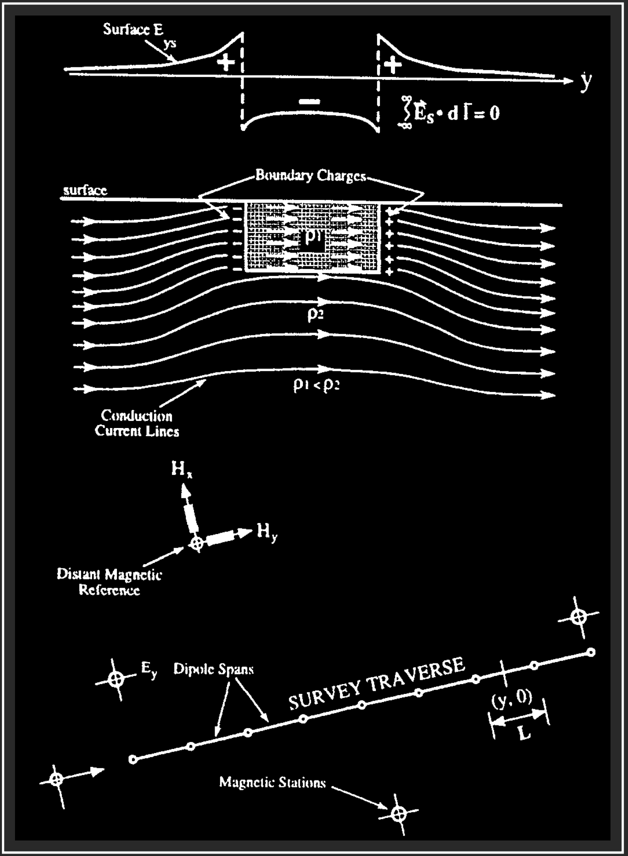

-Thus both Zxy and Zyx are zero-mean
-Zav = [Zxy – Zyx]/2 a logical background

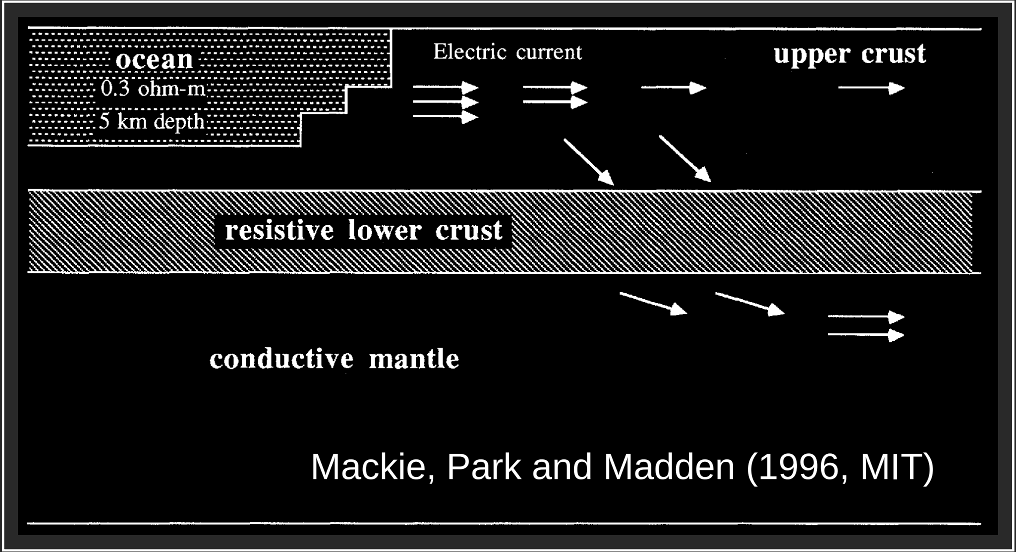

Mackie, Park and Madden (1996, MIT)

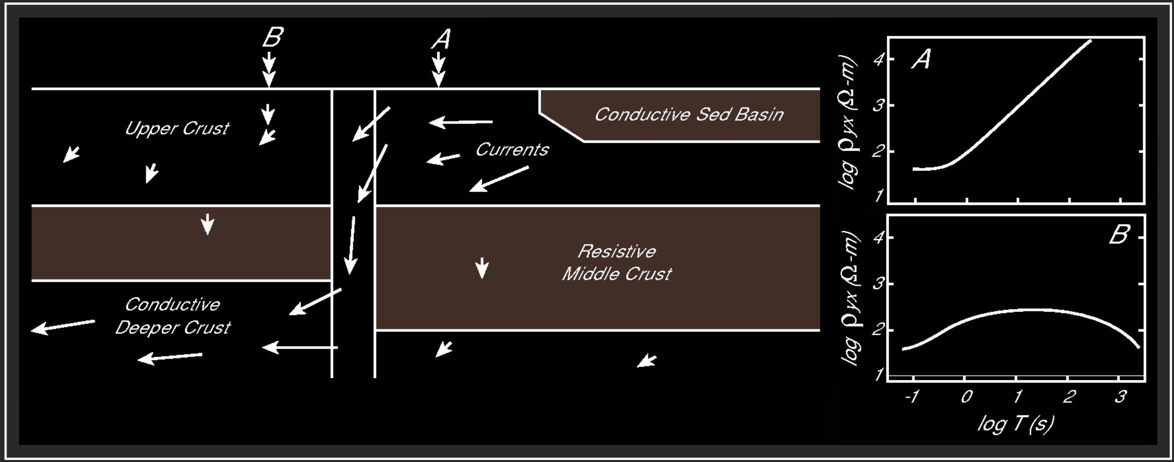

Vertical Current Channeling down Crustal-Scale Fault Zone

Crustal-Scale Breaks and Multiscale Magmatic/Hydrothermal Connections

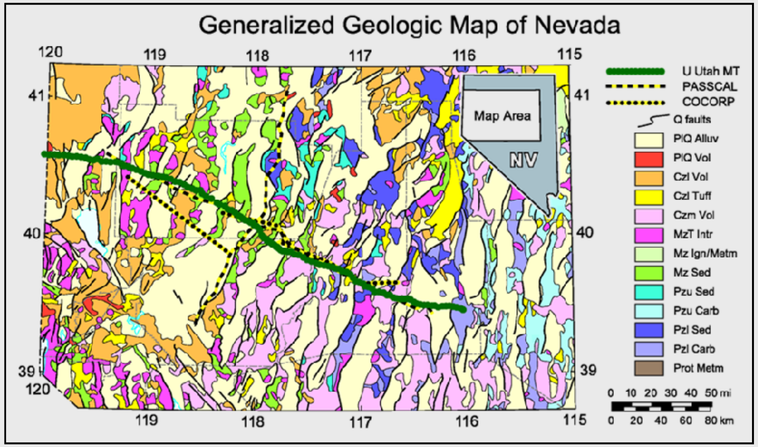

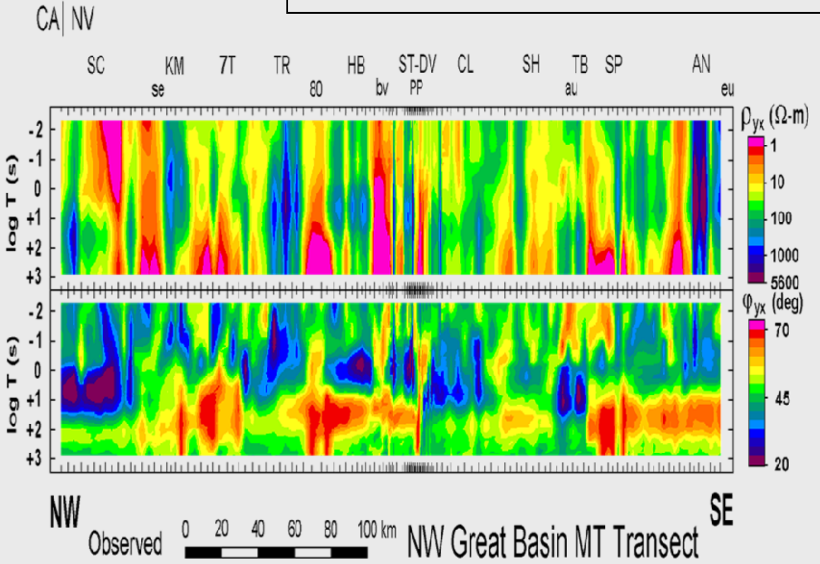

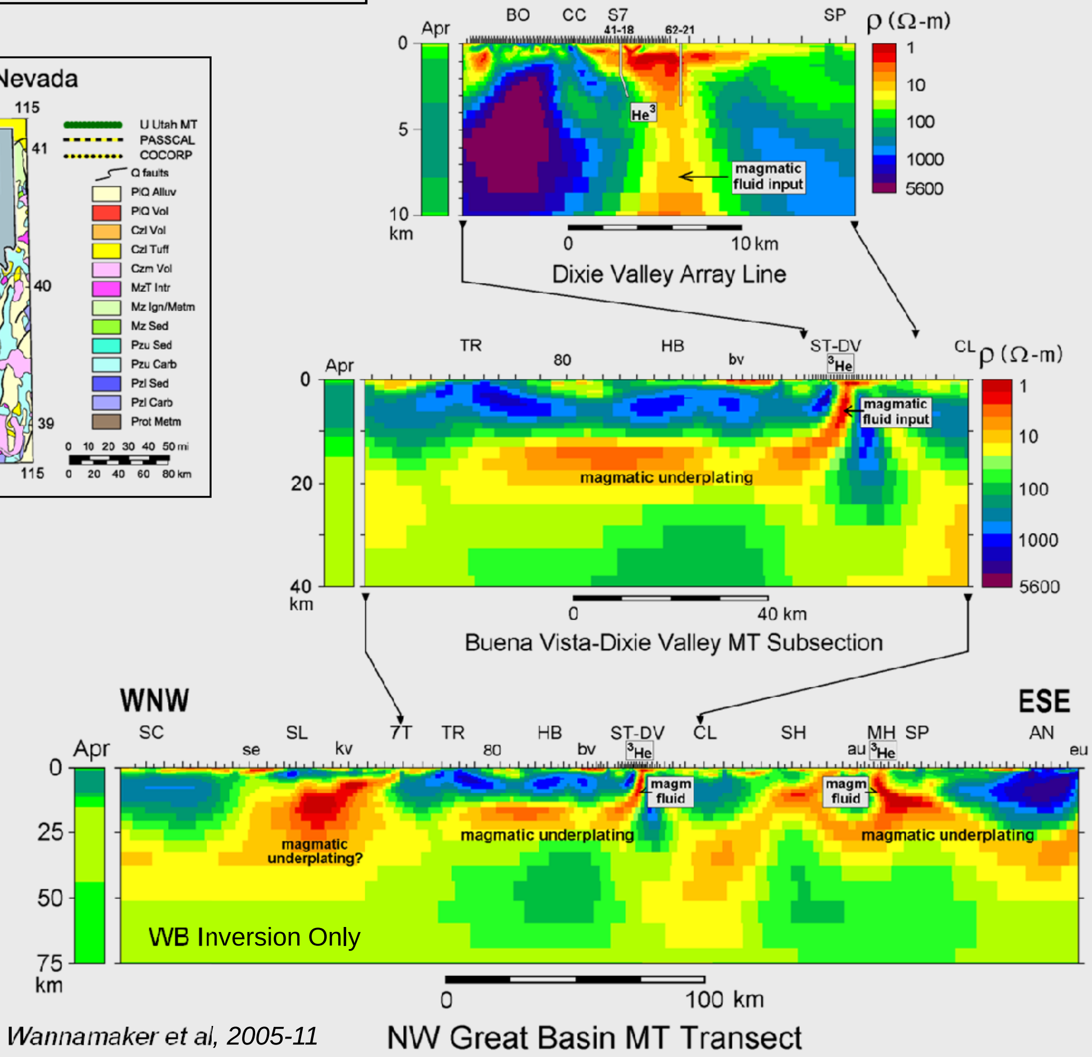

Wannamaker et al, 2005-11

Crustal-Scale Breaks and Multiscale Magmatic/Hydrothermal Connections

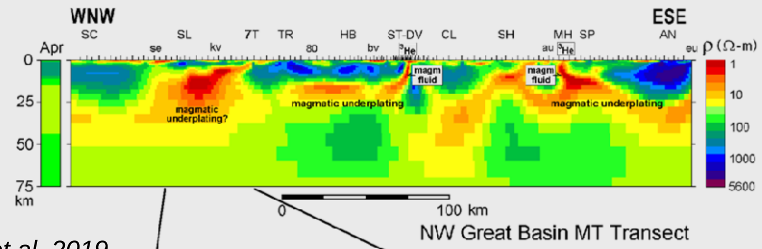

Wannamaker et al, 2019

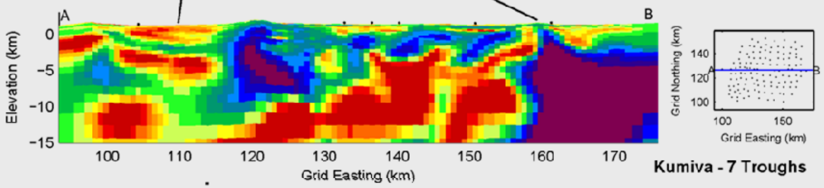

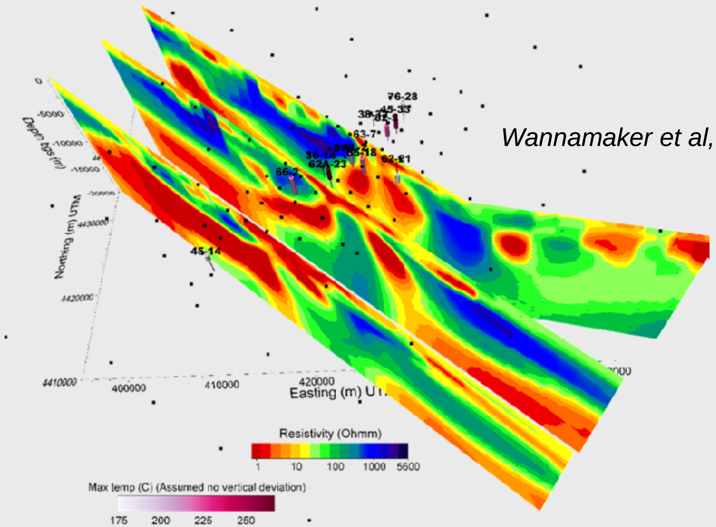

Wannamaker et al, 2013

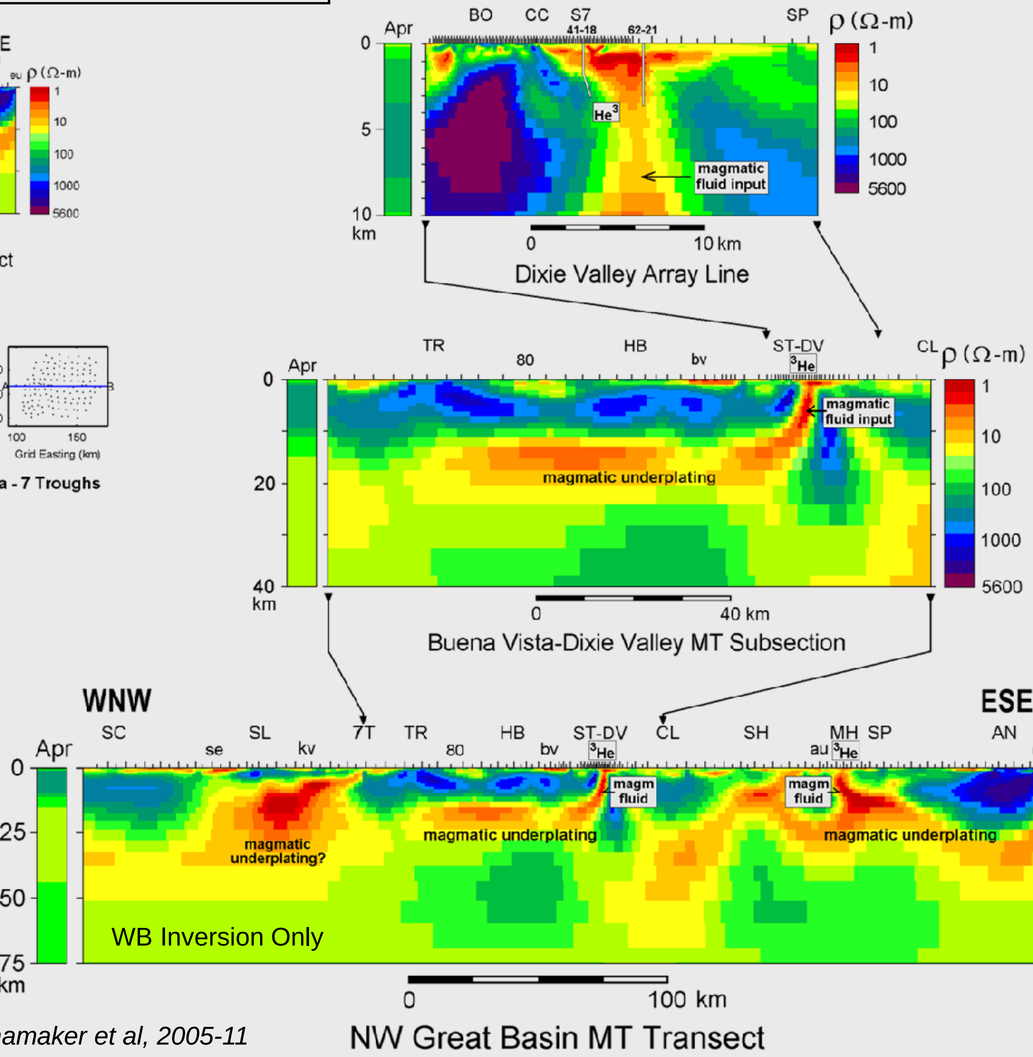

Wannamaker et al, 2005-11

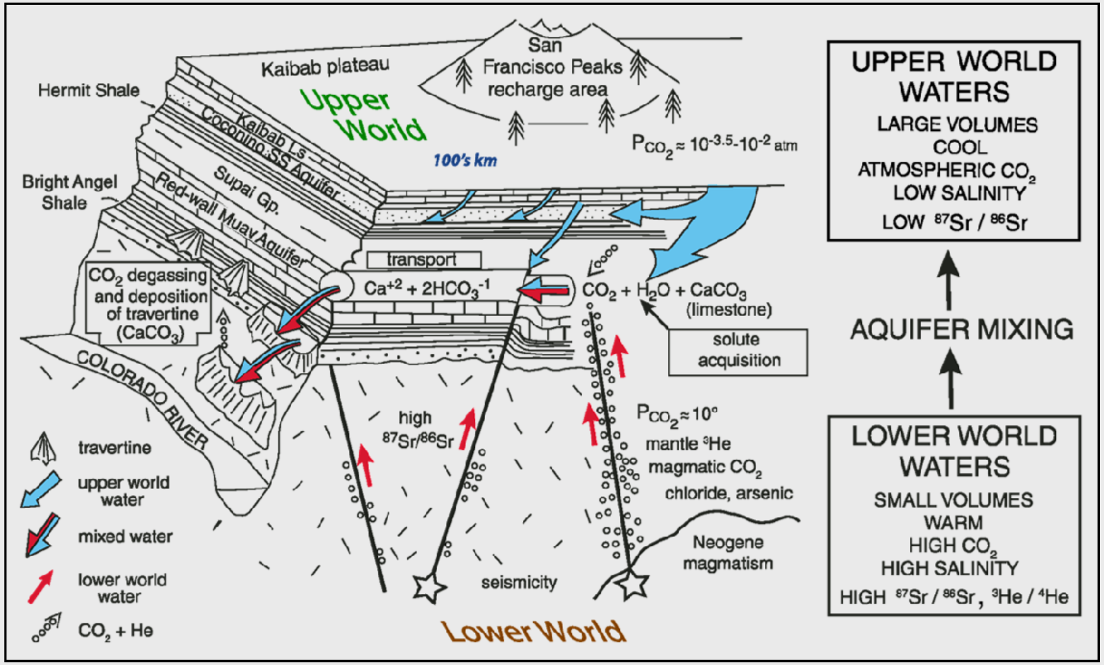

Multiscale Magmatic/Hydrothermal Connections

Grand Canyon Hydrological Model
(Crossey and Karlstrom, 2012)

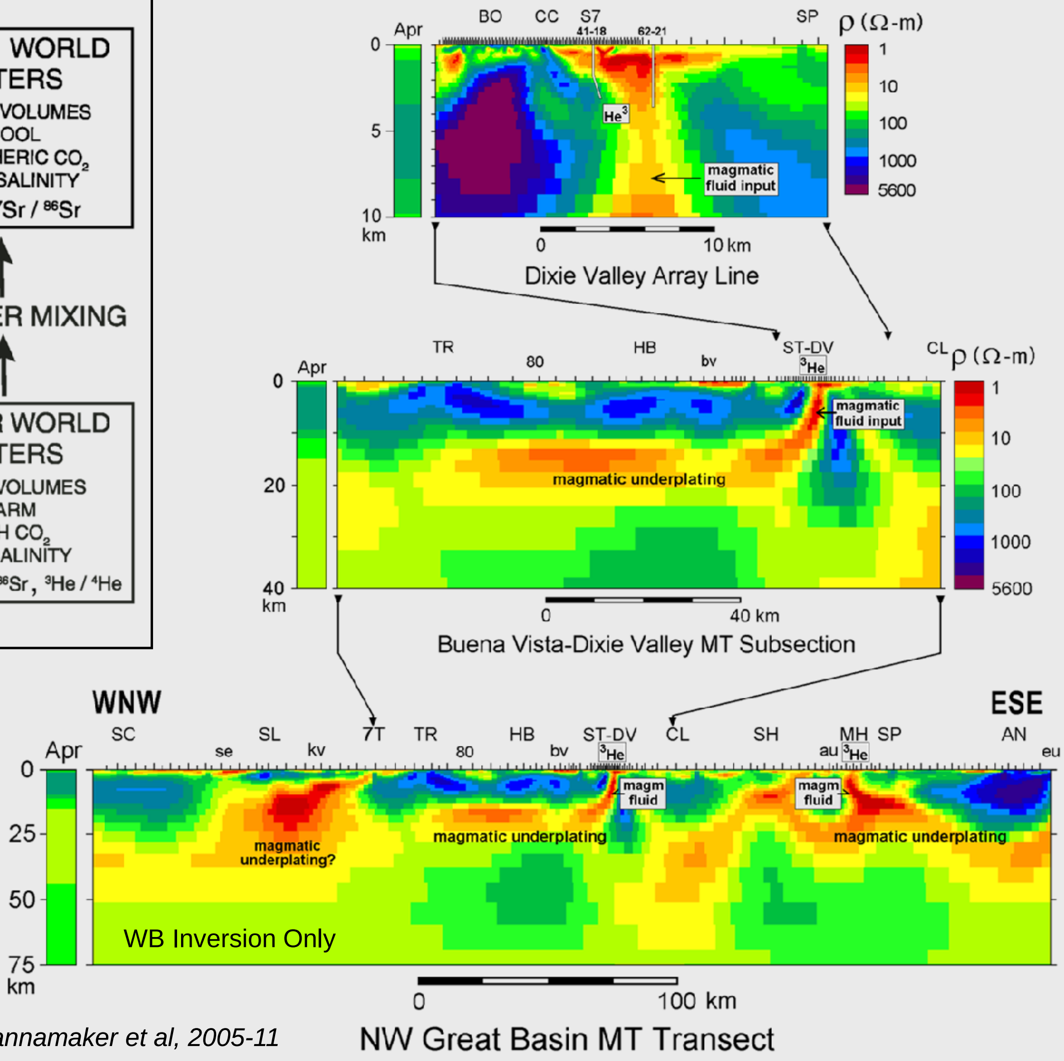

Wannamaker et al, 2005-11

Exhumed Crustal Sections
(Fountain and Salisbury, 1981)

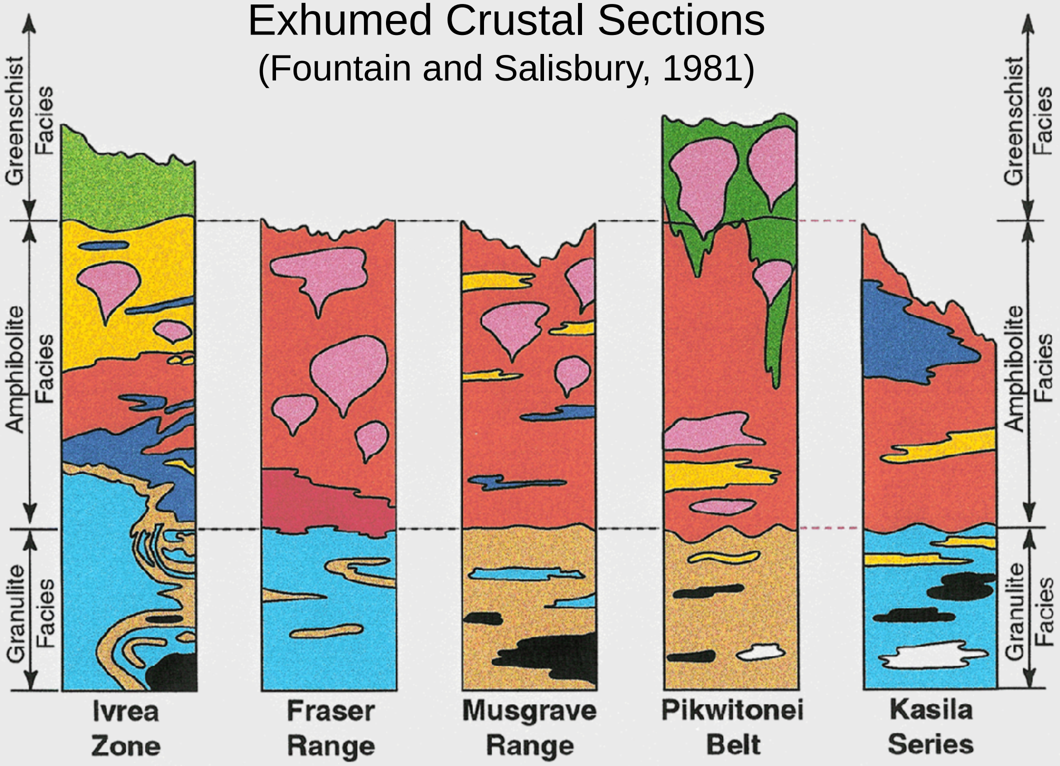

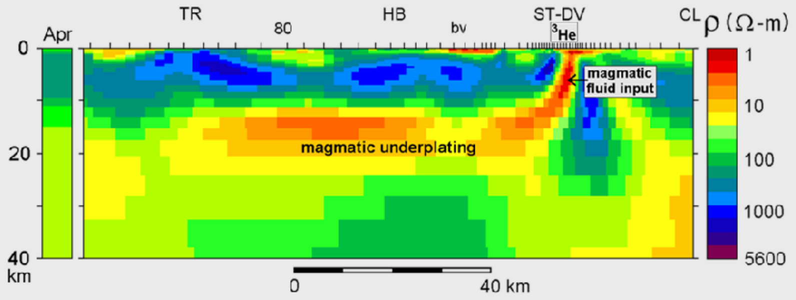

Buena Vista-Dixie Valley MT Subsection

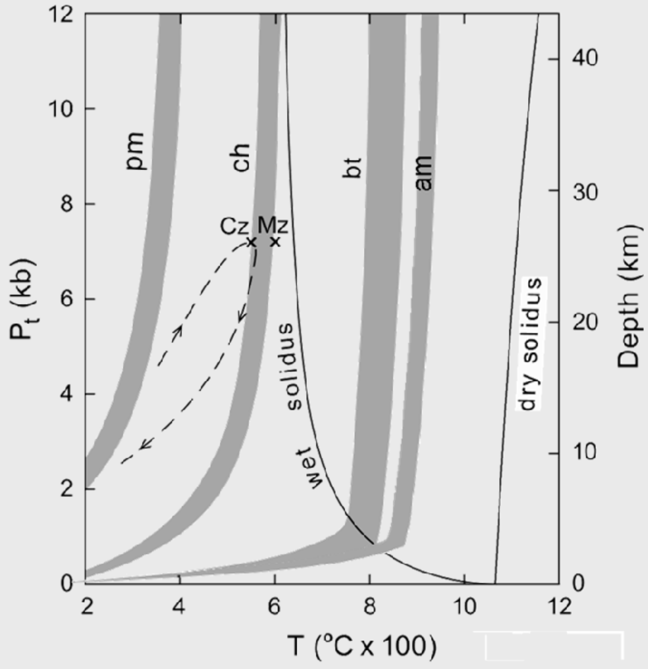

Diorite-H2O petrogenetic grid

- Free water not compatible with granulite-upper amphibolite facies- resorbed to more amph/biotite
- Any present fluid must be of low a(H2O)
- Complex salts may provide a mechanism
- Comment/Reply Yardley (1997, 2000), Wannamaker (2000)

Exhumed Crustal Sections
(Fountain and Salisbury, 1981)

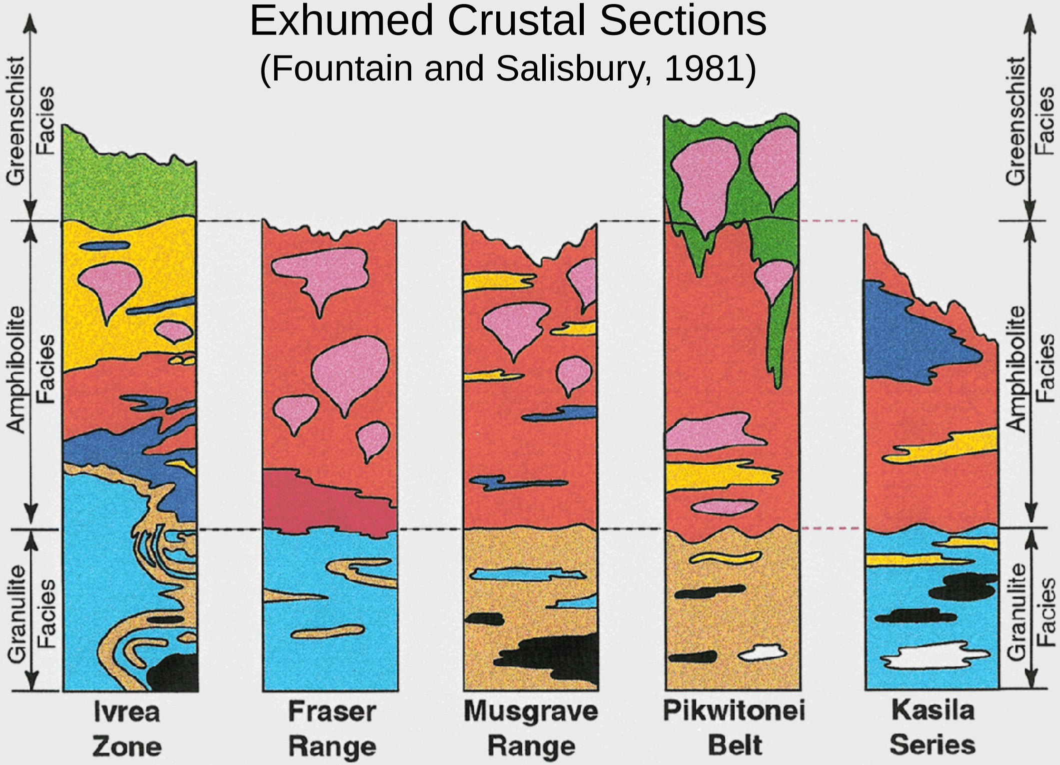

- Free water not compatible with granulite-upper amphibolite facies- resorbed to more amph/biotite
- Any present fluid must be of low a(H2O)
- Complex salts may provide a mechanism
- Comment/Reply Yardley (1997, 2000), Wannamaker (2000)

Aranovich and Newton (1997)

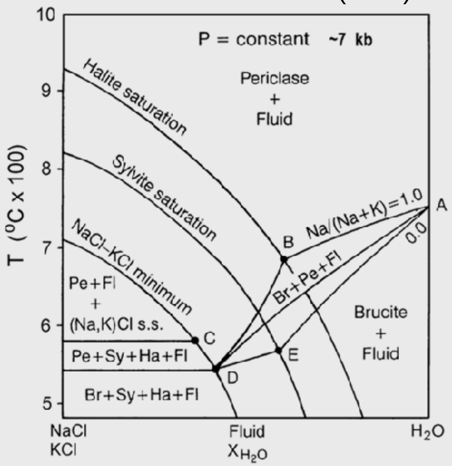

Complex salts reduce T of last fluid

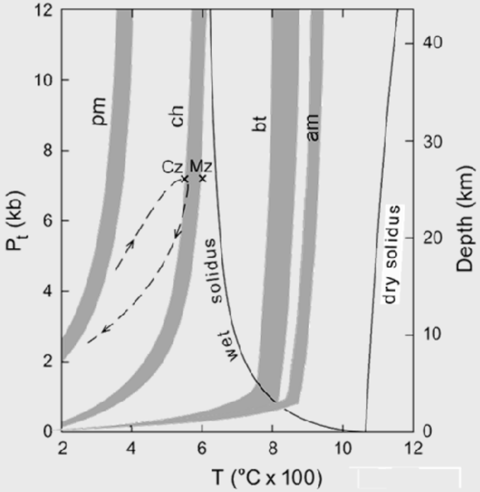

Diorite-H2O petrogenetic grid

Exhumed Crustal Sections
(Fountain and Salisbury, 1981)

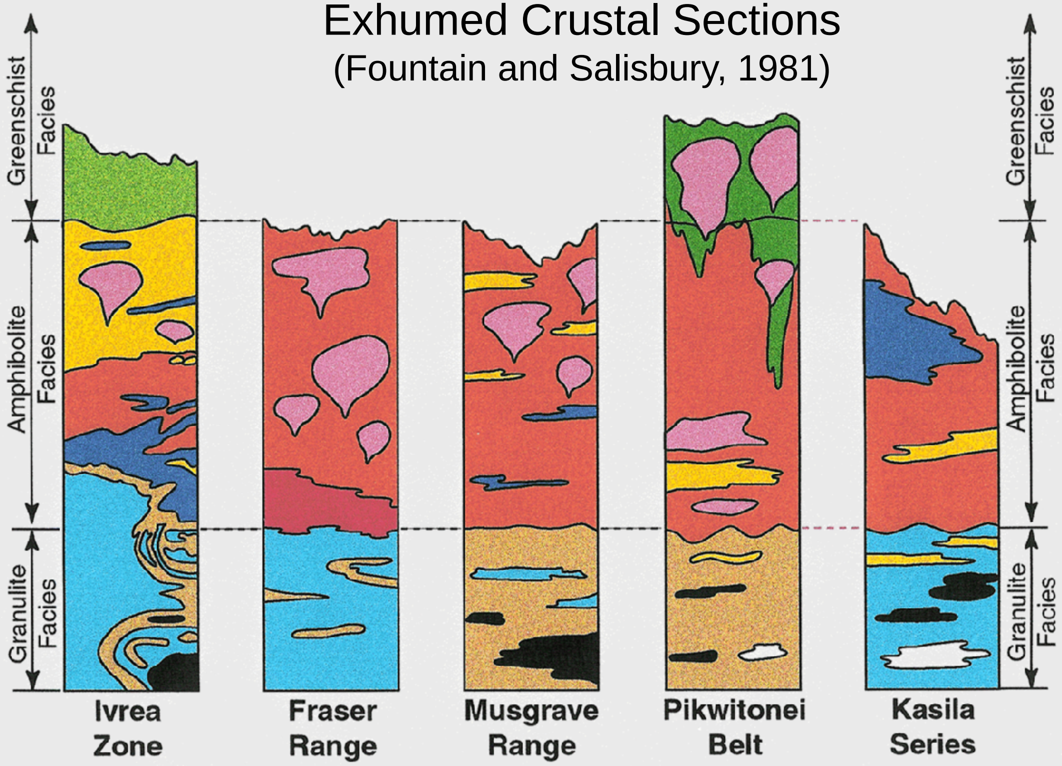

- Free water not compatible with granulite-upper amphibolite facies- resorbed to more amph/biotite
- Any present fluid must be of low a(H2O)
- Complex salts may provide a mechanism
- Comment/Reply Yardley (1997, 2000), Wannamaker (2000)

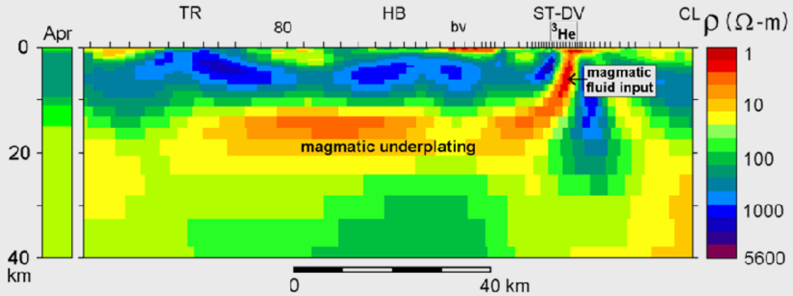

Buena Vista-Dixie Valley MT Subsection

Aranovich and Newton (1997)

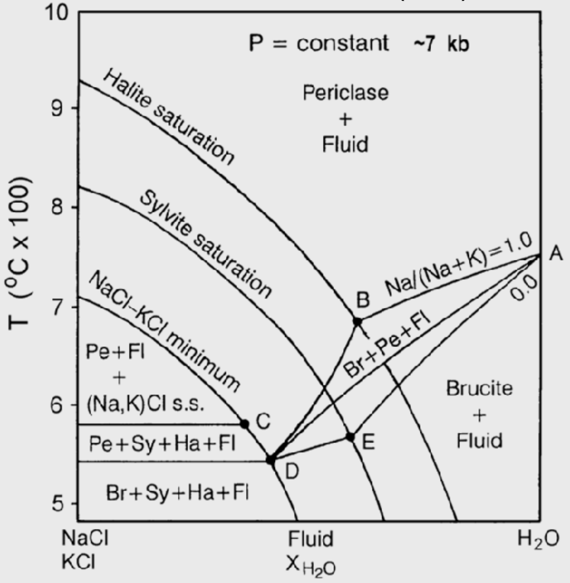

Complex salts reduce T of last fluid

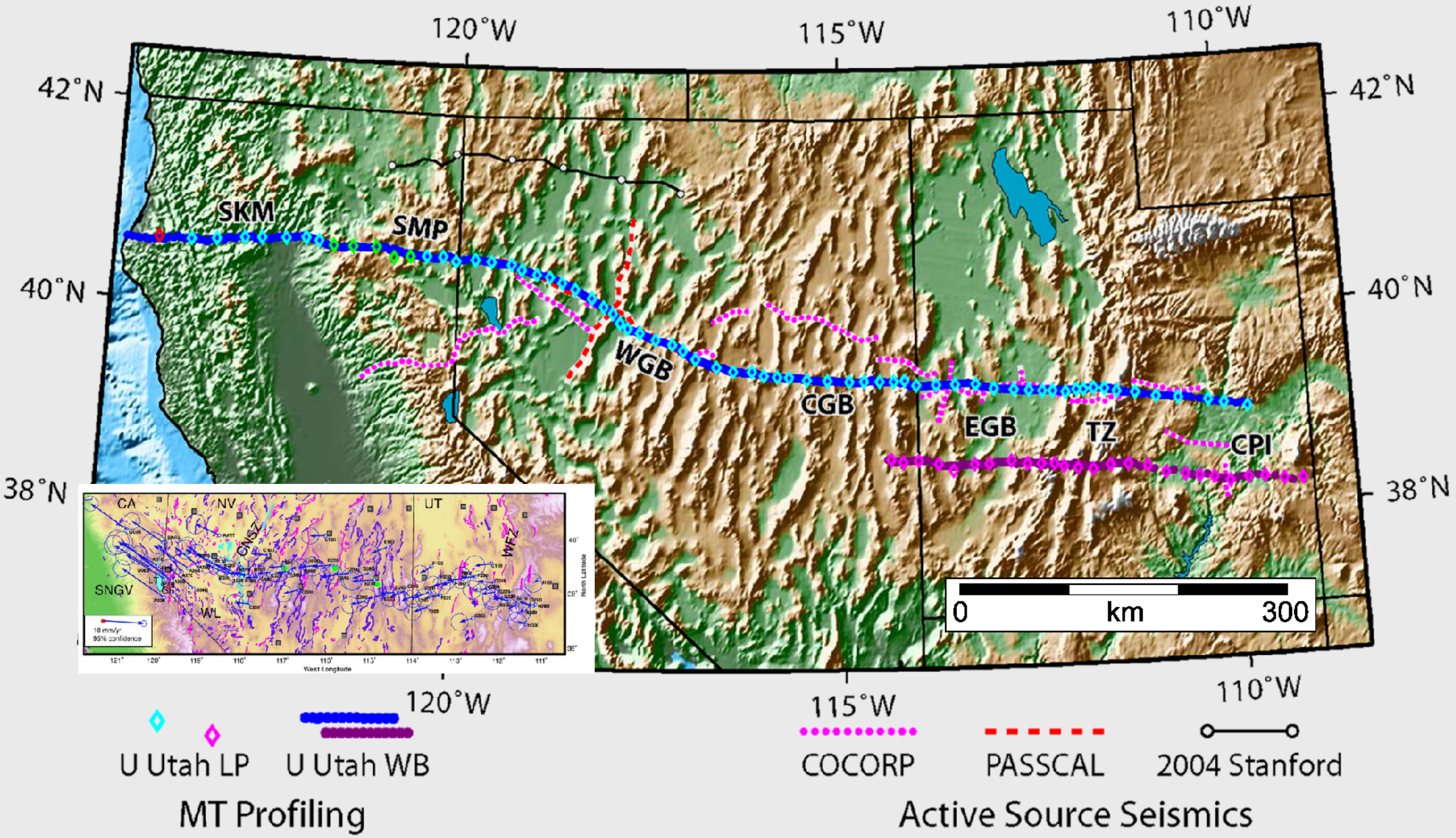

S Klamath Mtns – Great Basin – Colorado Plateau MT

Approx. coincident with COCORP, PASSCAL seismic profiling

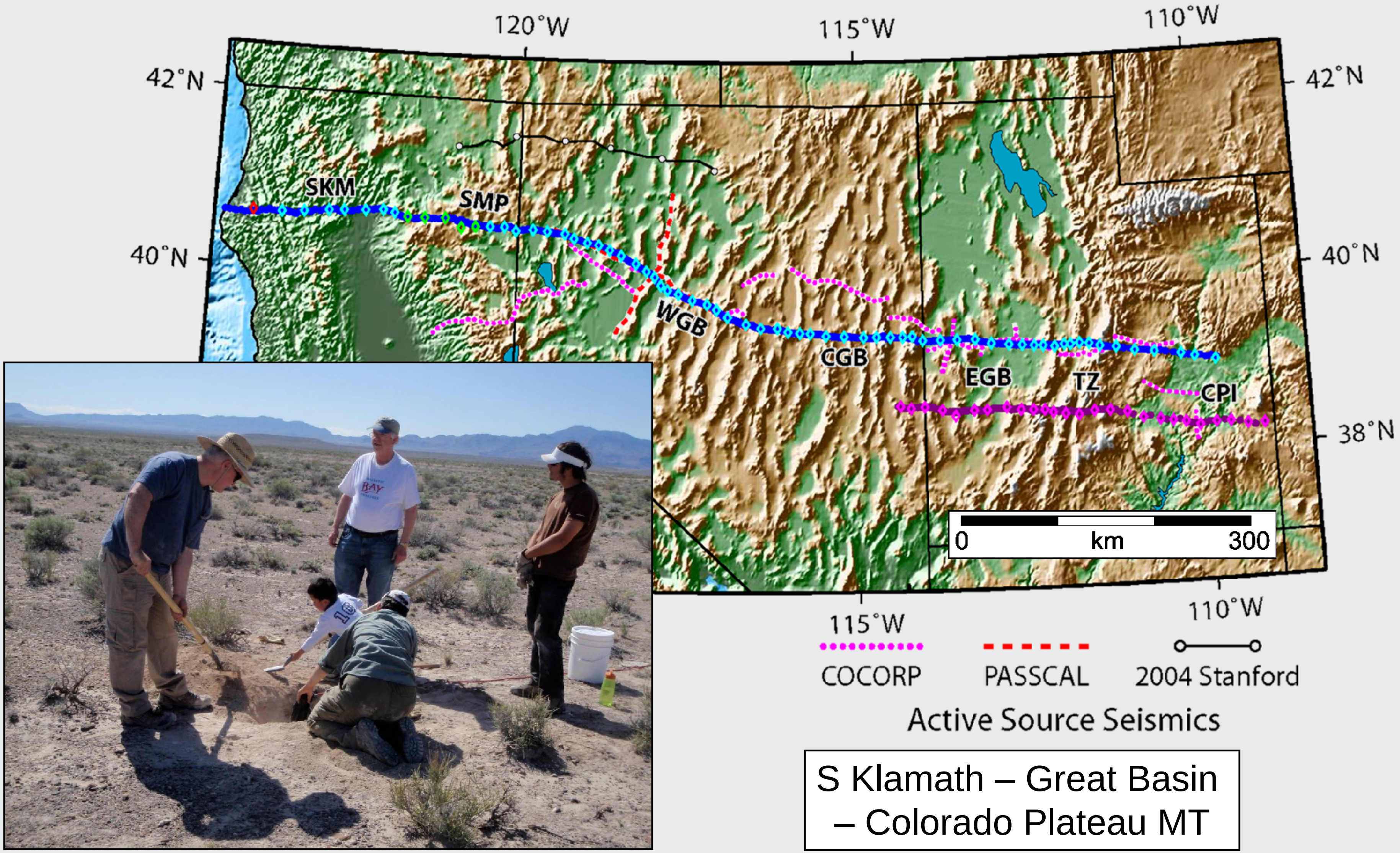

S Klamath – Great Basin – Colorado Plateau MT

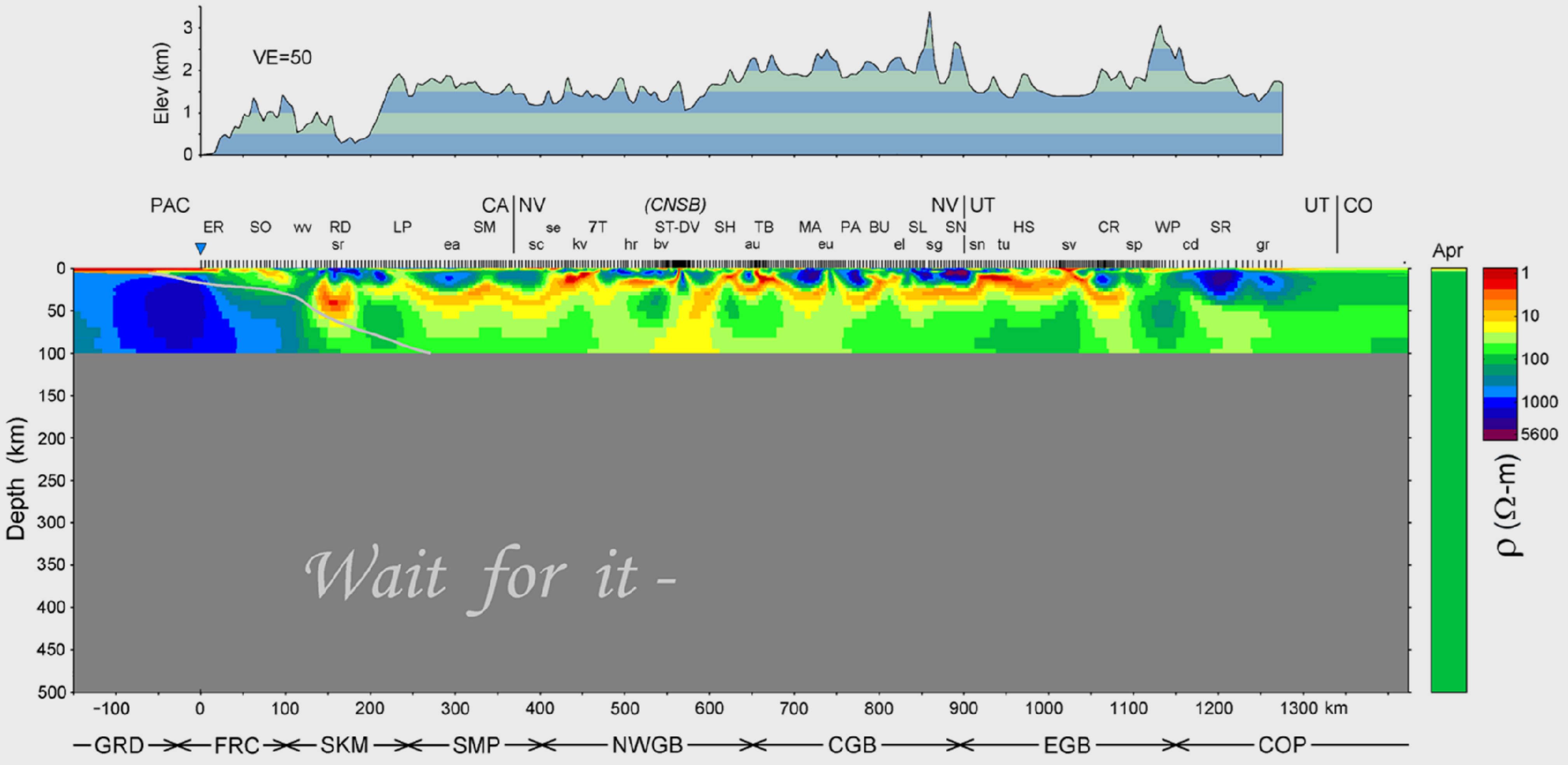

Klamath - S Modoc - Great Basin - Colorado Plateau
MT Transect (~40 N lat.)

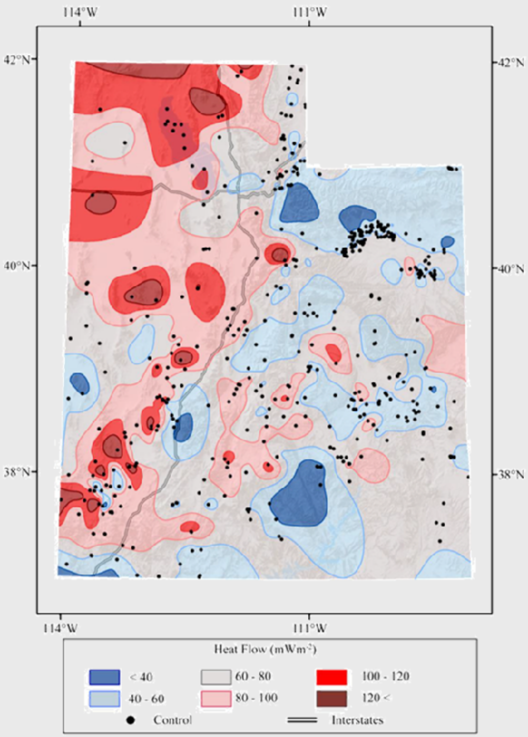

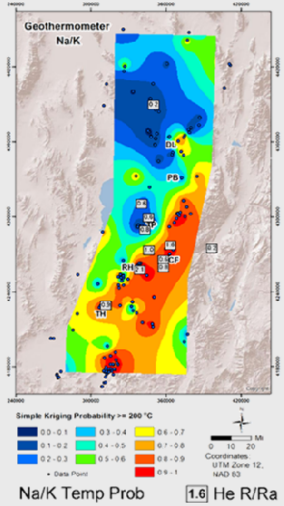

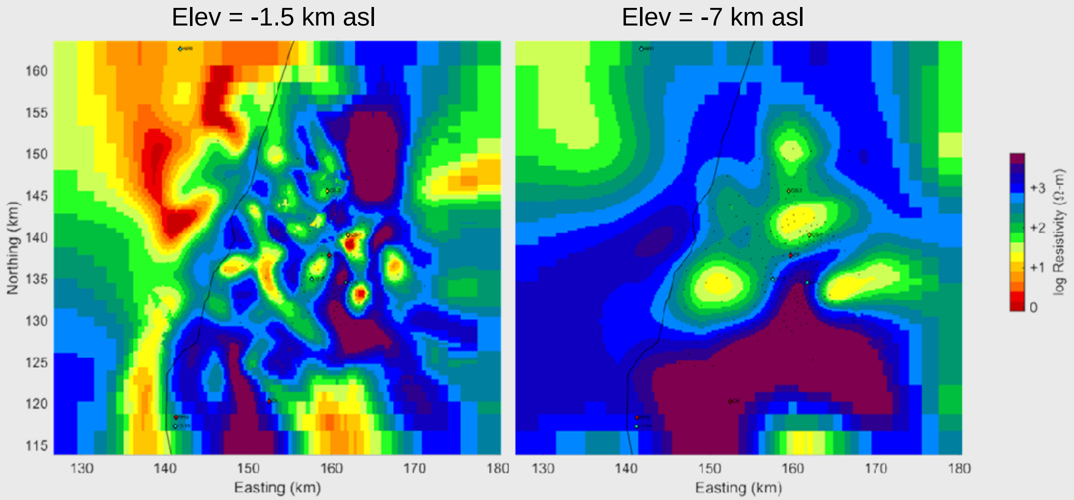

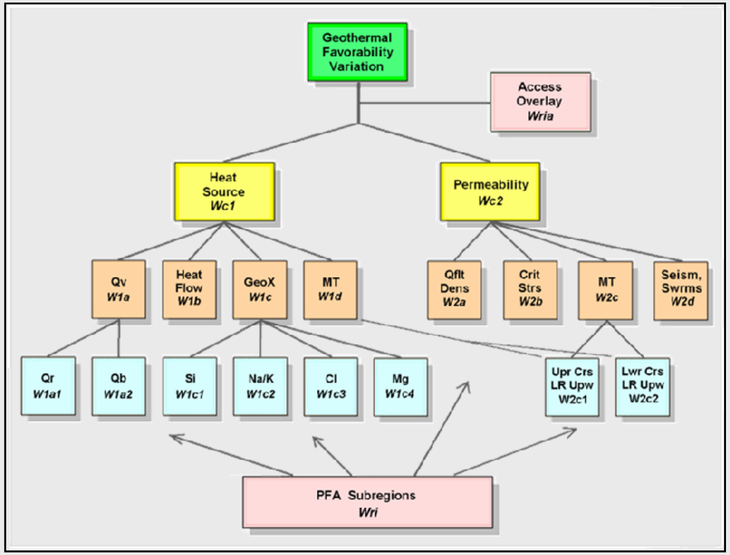

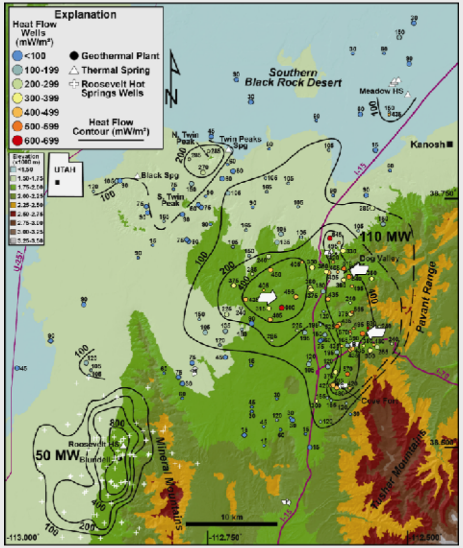

Multi-Criteria Decision Making (MCDM) Implementation for Geothermal Prospectivity

(Wannamaker et al., 2017)

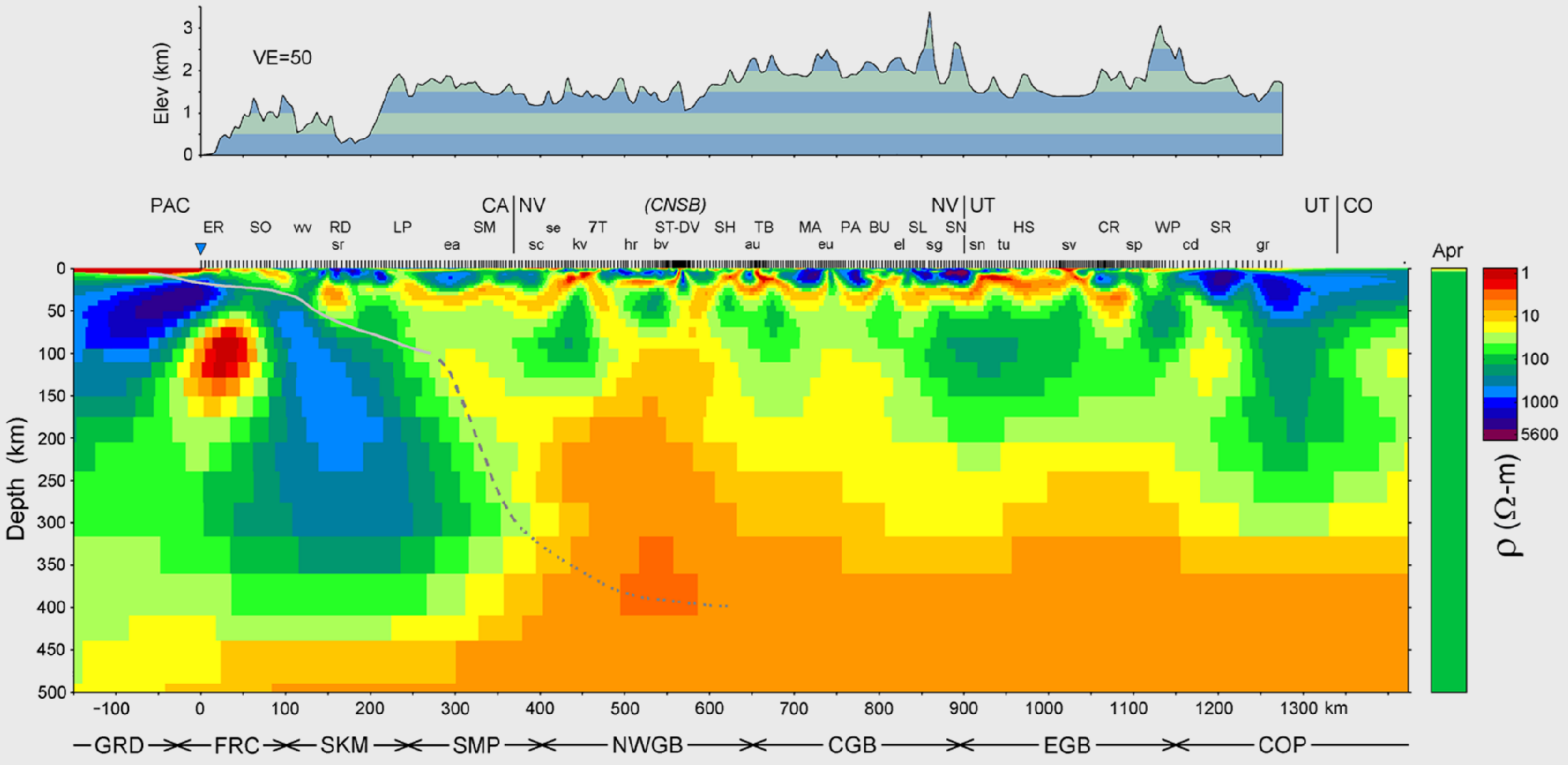

Klamath - S Modoc - Great Basin - Colorado Plateau
MT Transect (~40 N lat.)

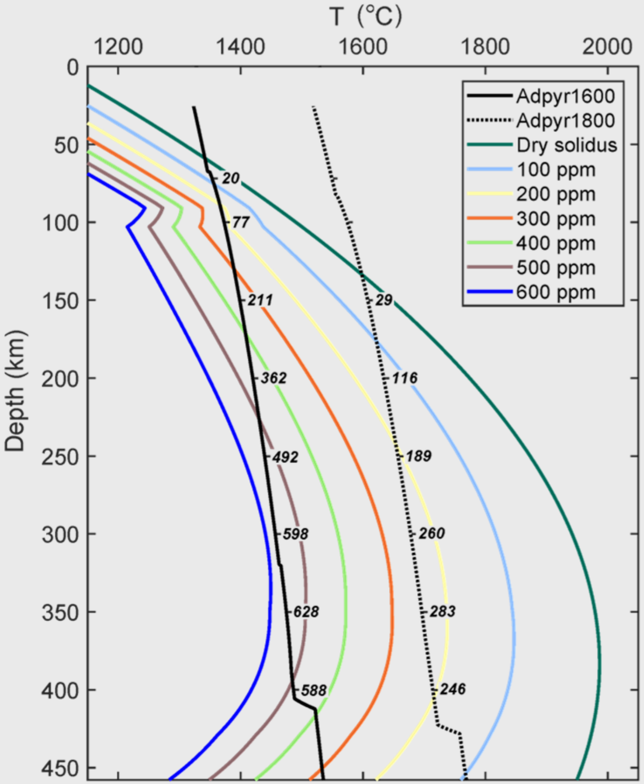

Hirschmann et al (2009, PEPI)
Stixrude and Lithgow-Bertelloni (2011, GJI)

Novella et al (2014, EPSL)

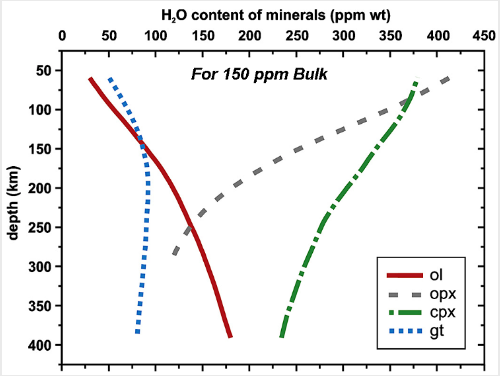

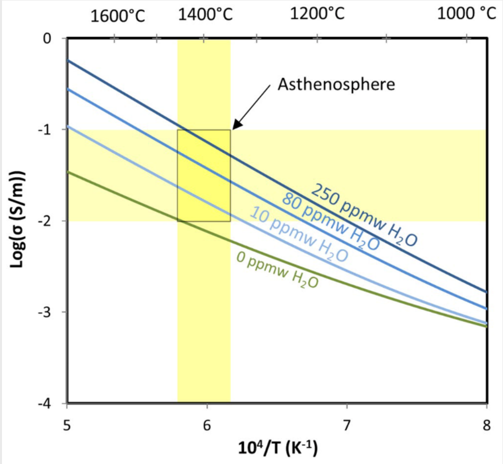

Novella et al (2017, Sci Rpt)

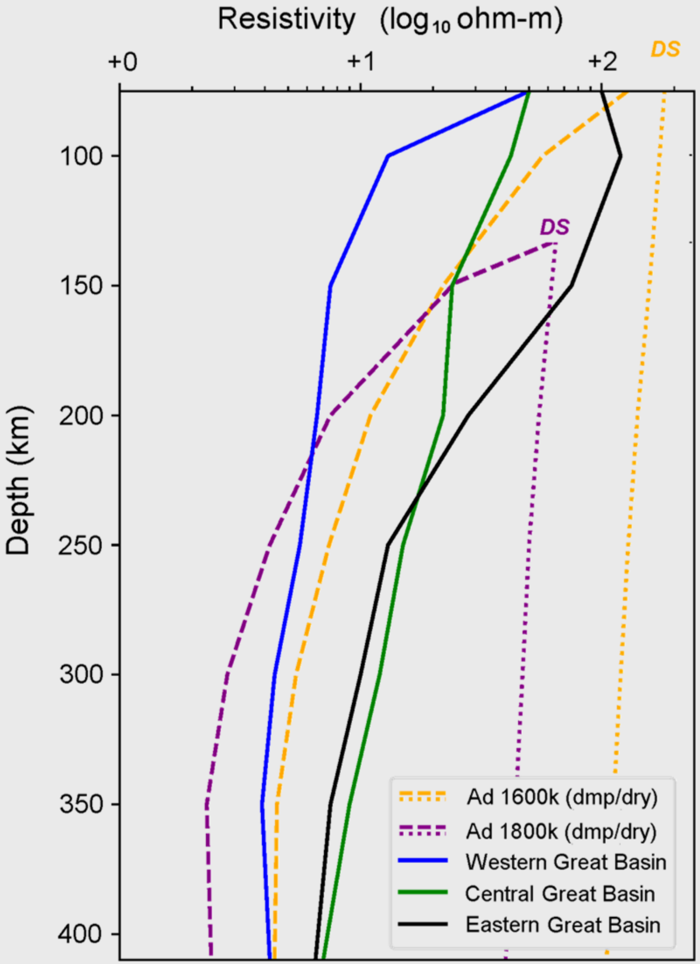

Electrical conductivity and Paleo-Proterozoic foredeeps

D.E. Boerner, R.D. Kurtz, and J.A. Craven

JOURNAL OF GEOPHYSICAL RESEARCH, VOL. 101, NO. B6, 1996

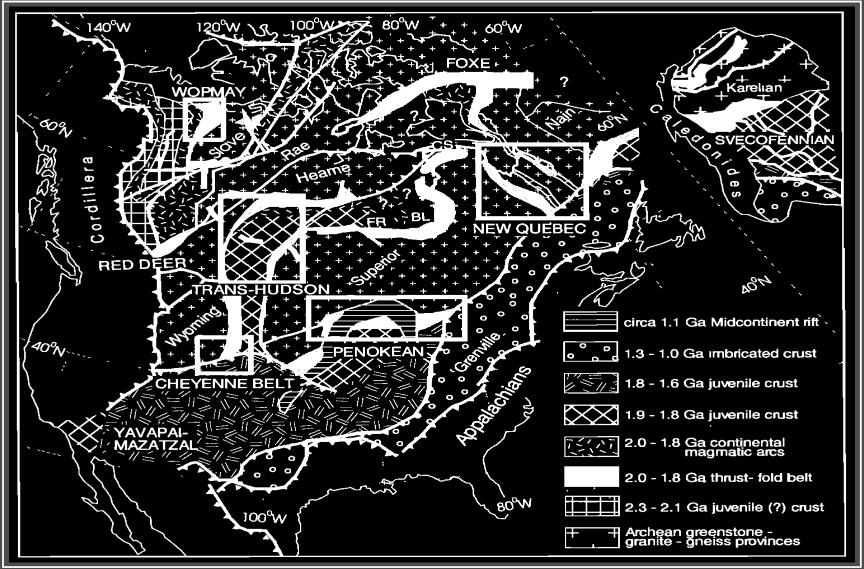

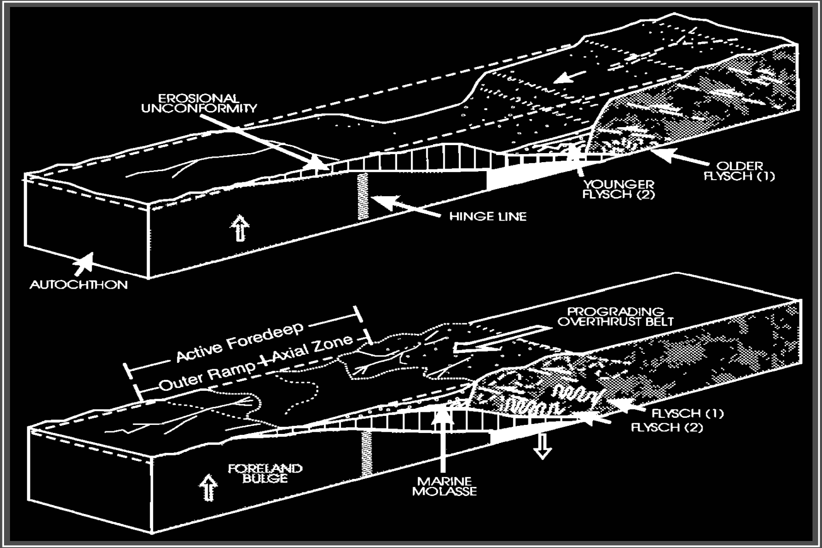

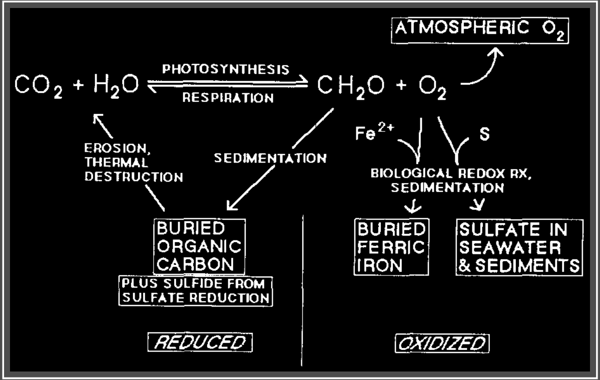

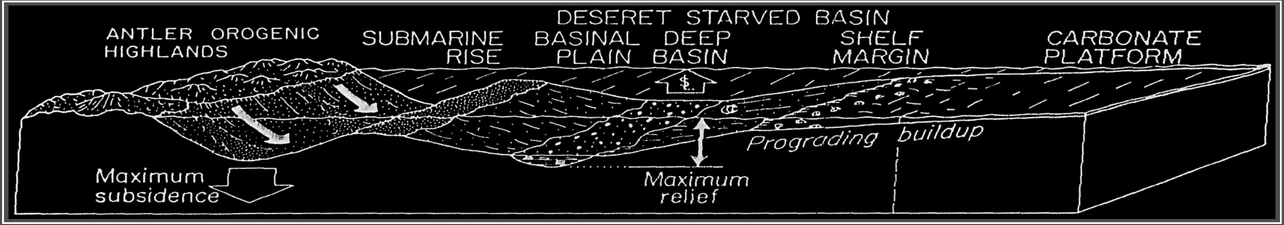

Cyanobacterial O production
← and oC-Sd sequestration
Des Marais (1994)

C-S concentration in starved basins
Sandberg and Gutschick (1983)

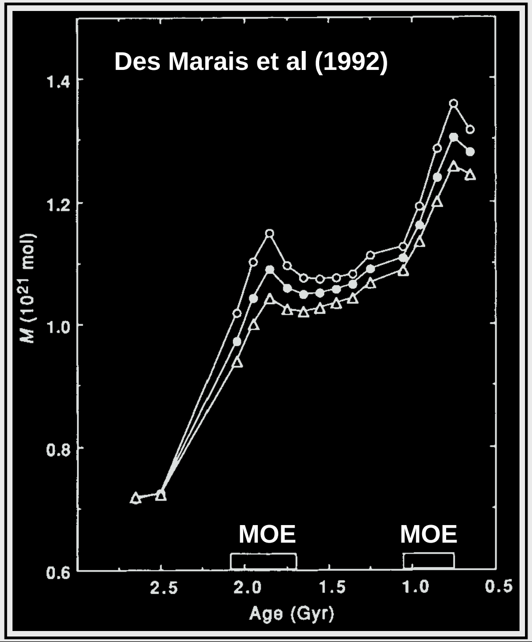

oC-Sd global primary production

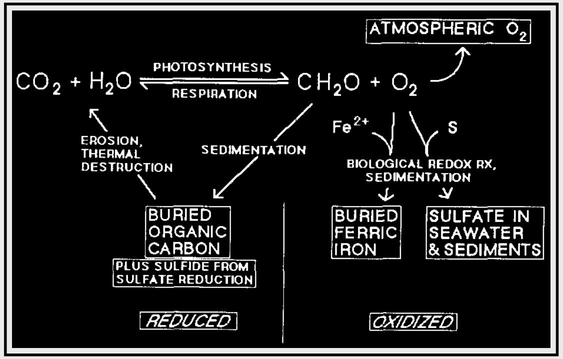

oC-Sd sequestration

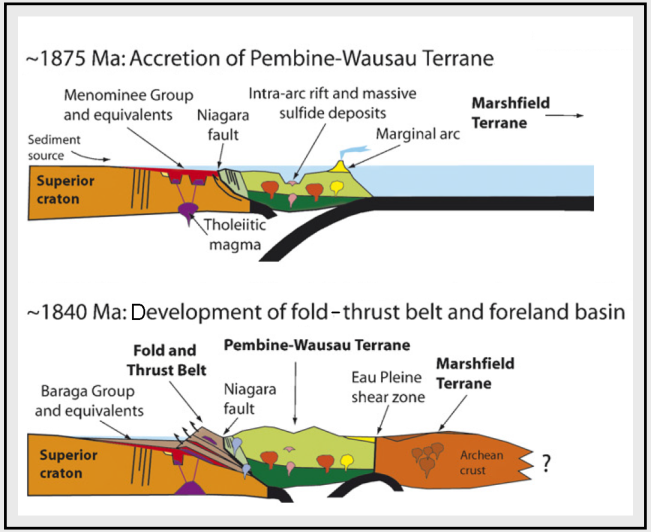

Mod from Schulz and Cannon (2007)

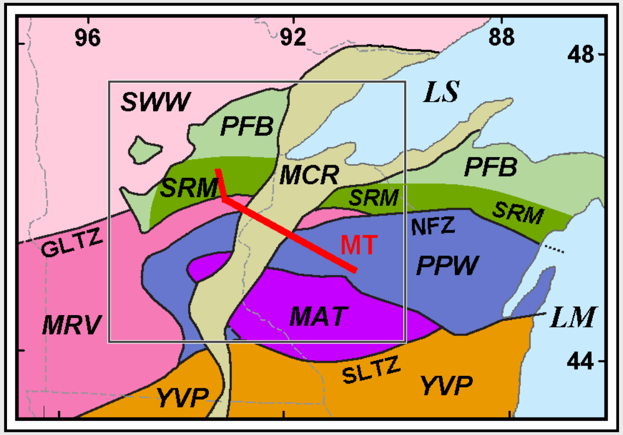

Mod from Southwick (2014)

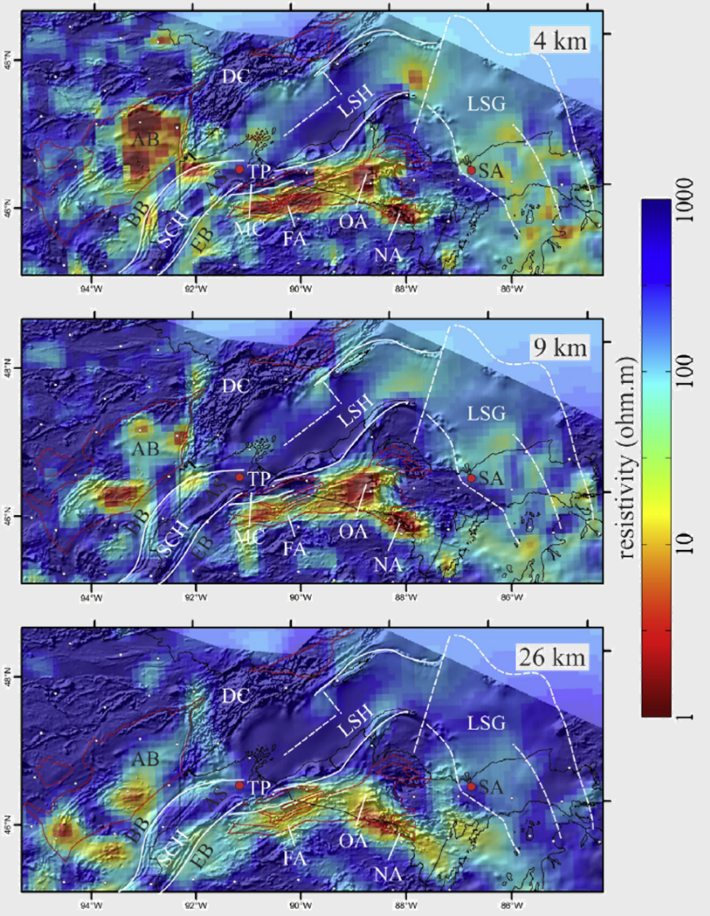

Bedrosian (2016)

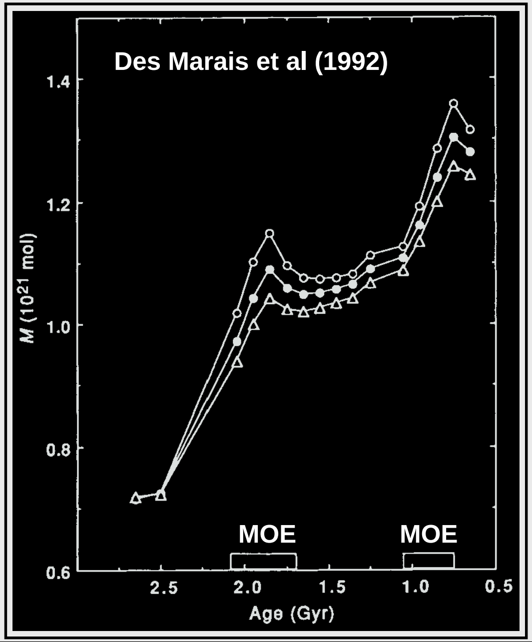

oC-Sd global primary production

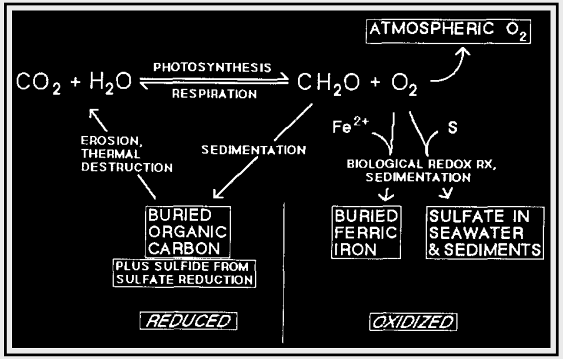

oC-Sd sequestration

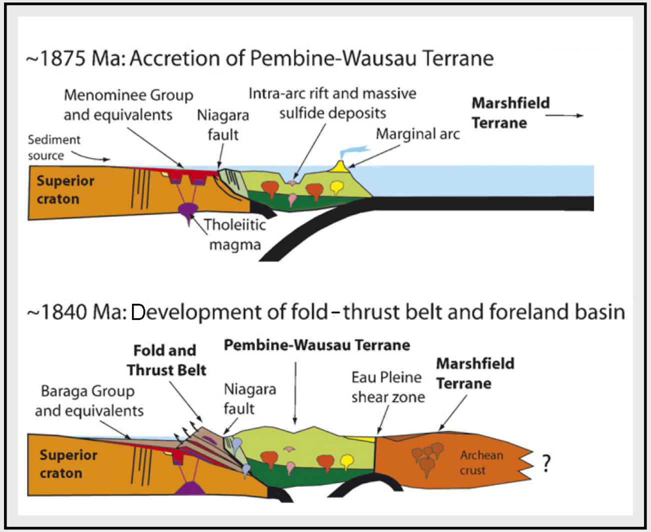

Mod from Schulz and Cannon (2007)

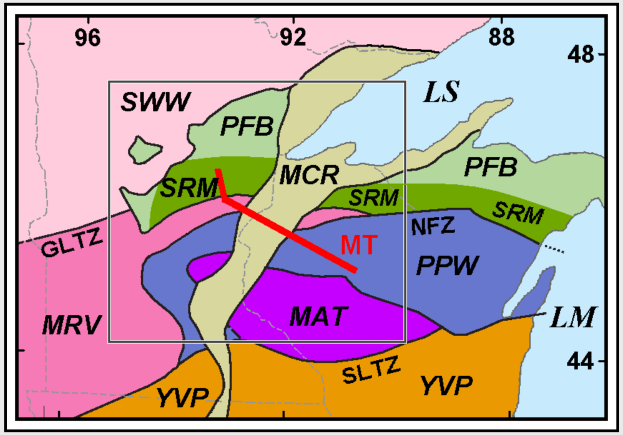

Mod from Southwick (2014)

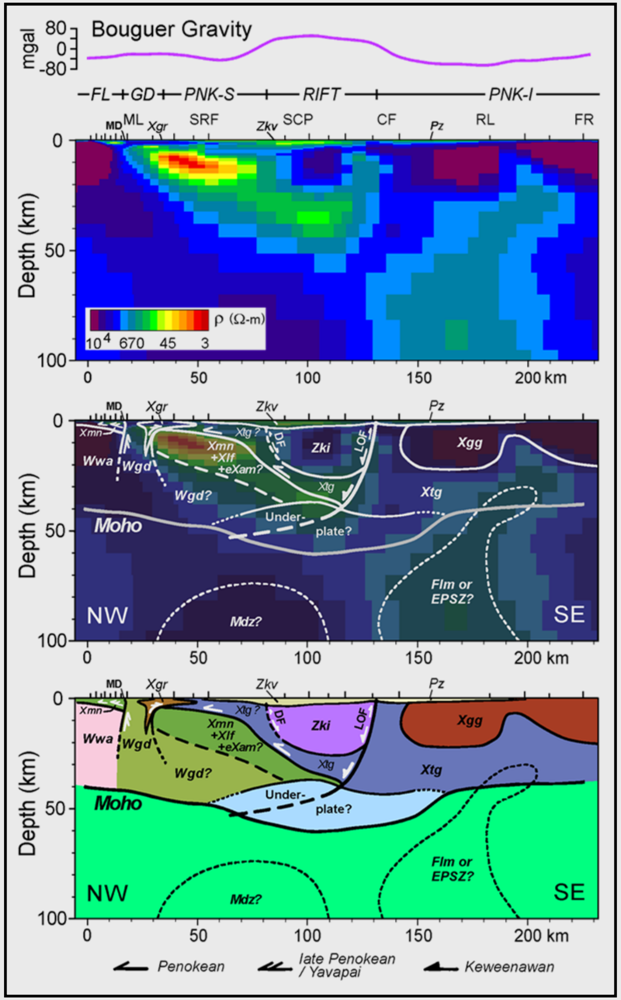

Wunderman et al. (2018)

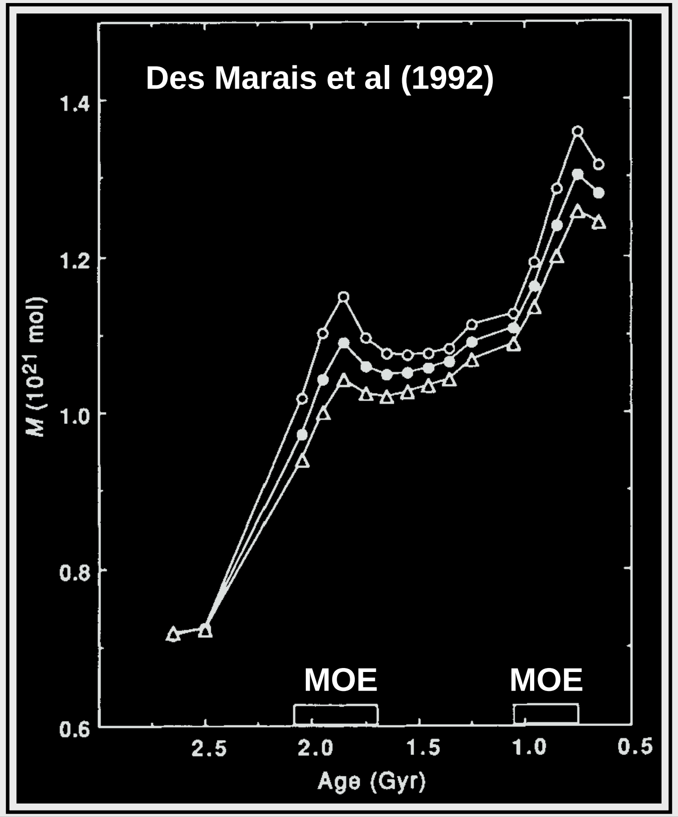

oC-Sd global primary production

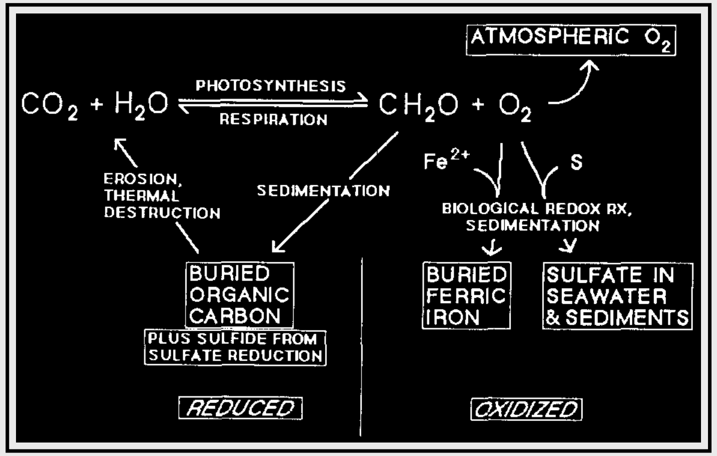

oC-Sd sequestration

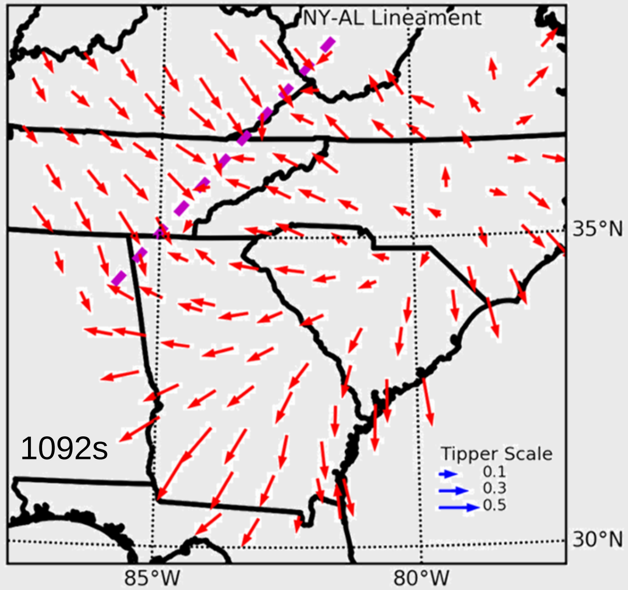

Murphy and Egbert (2017)

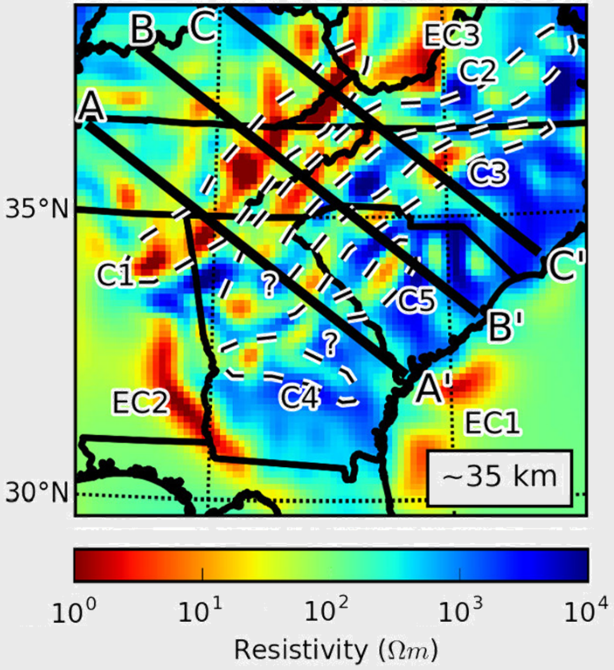

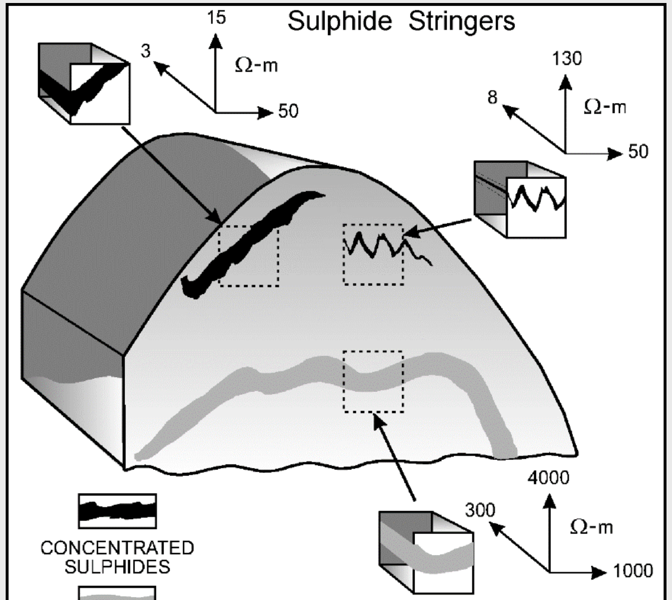

Jones et al. (JGG,1997)
Sulfide Stringers

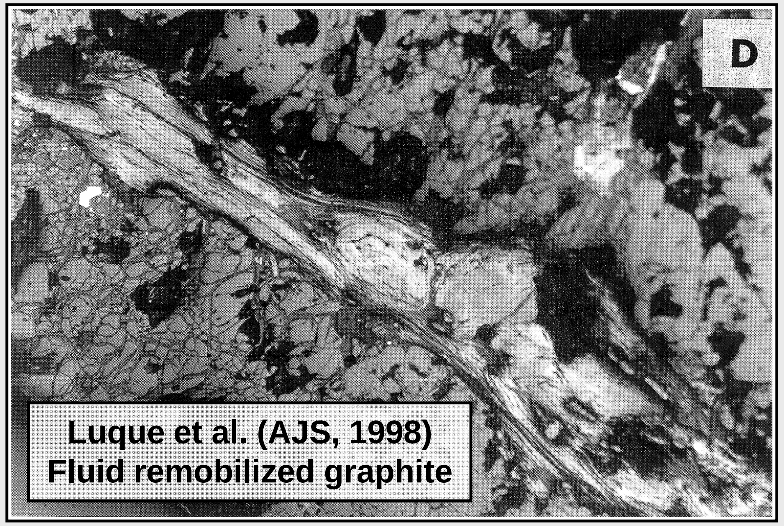

Luque et al. (AJS, 1998)
Fluid remobilized graphite

Graphite-sulfide textures in crustal-scale conductors

MT Recording Components For Polar Deployment

Induction Coil (Solenoid)

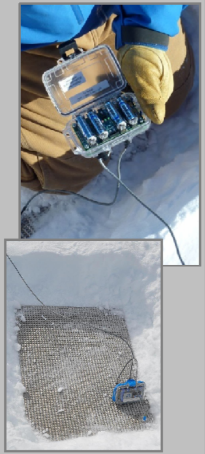

Ti Electrode w/ High-Z Preamp

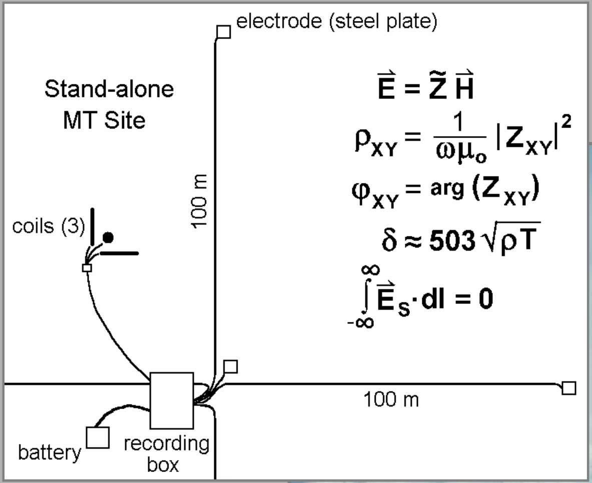

Sync'd MT recorders

Mount Erebus, Ross Island
(G. Hill, P. Wannamaker)

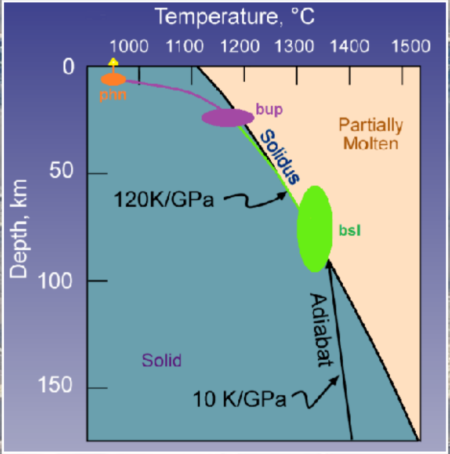

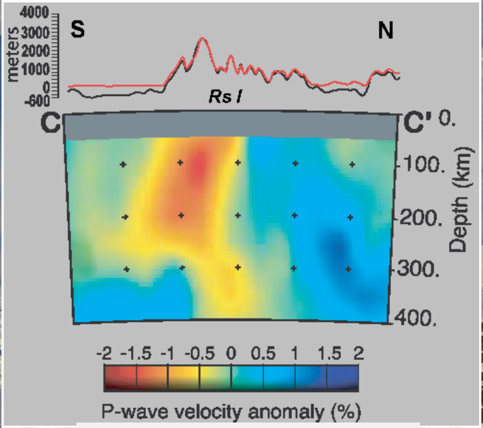

Watson et al (2006)

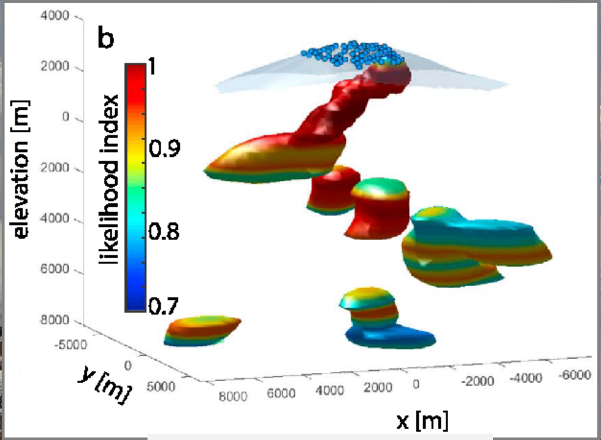

Blondel et al (2018)

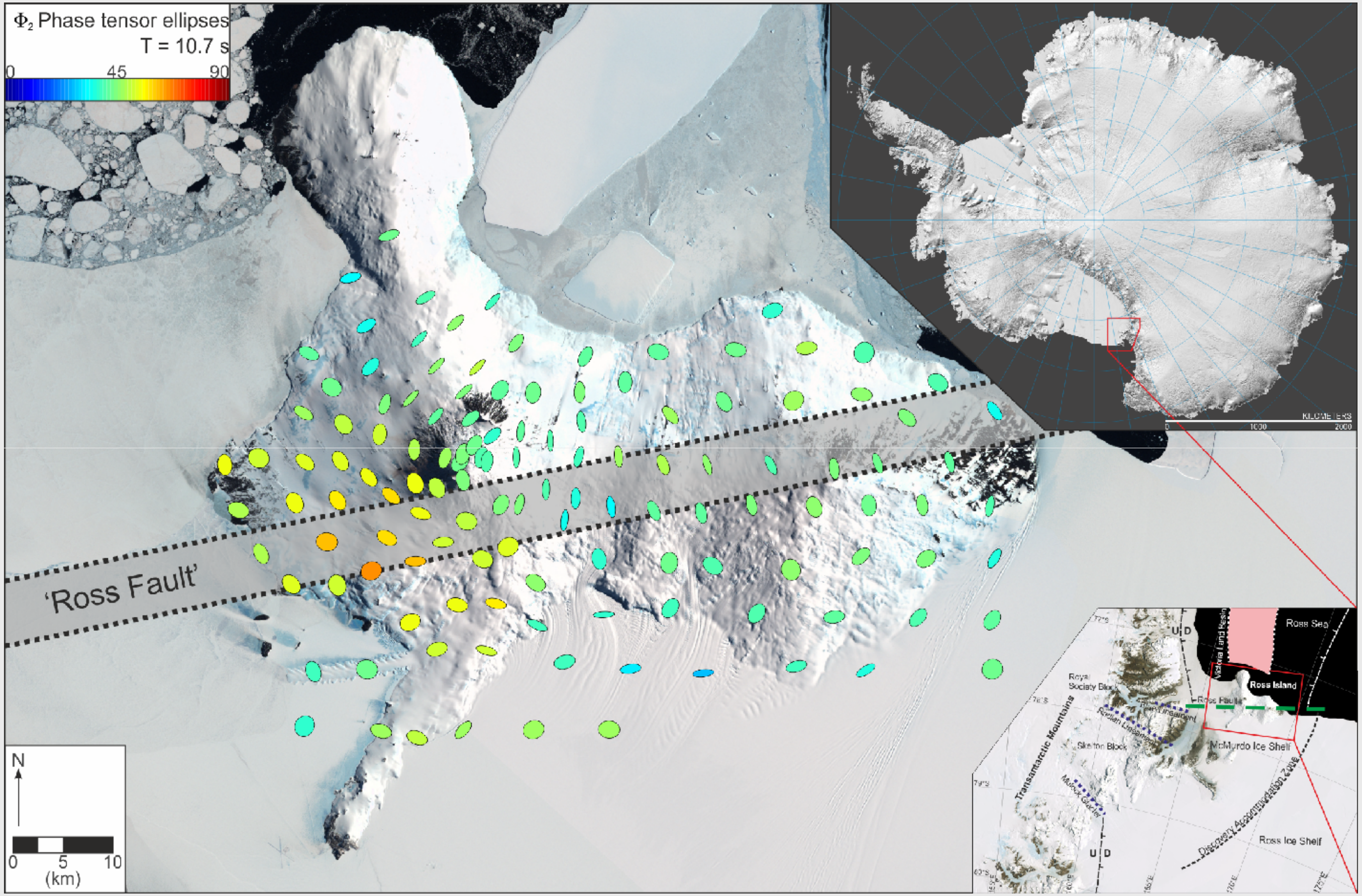

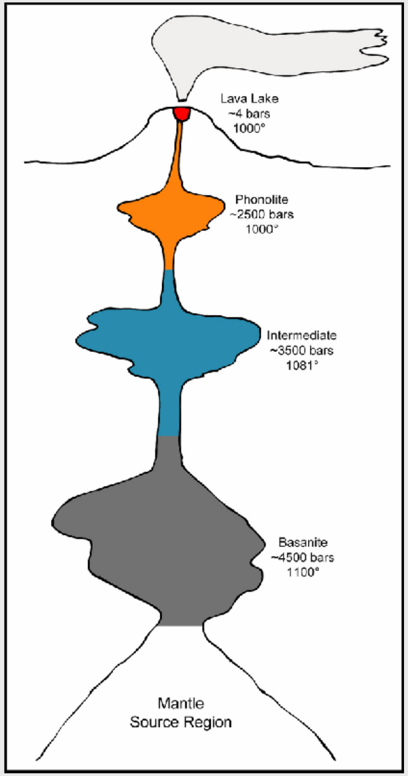

Mount Erebus Magma Source and Staging (Iacovino et al, 2015, after Oppenheimer, 2008)

Mt Erebus MT Field Campaign: NSF/USAP and RSNZ/AntNZ

Hill, Wannamaker, Maris, Stodt, Kordy, Wallin, Unsworth, Bedrosian, Uhlmann (2014-7)

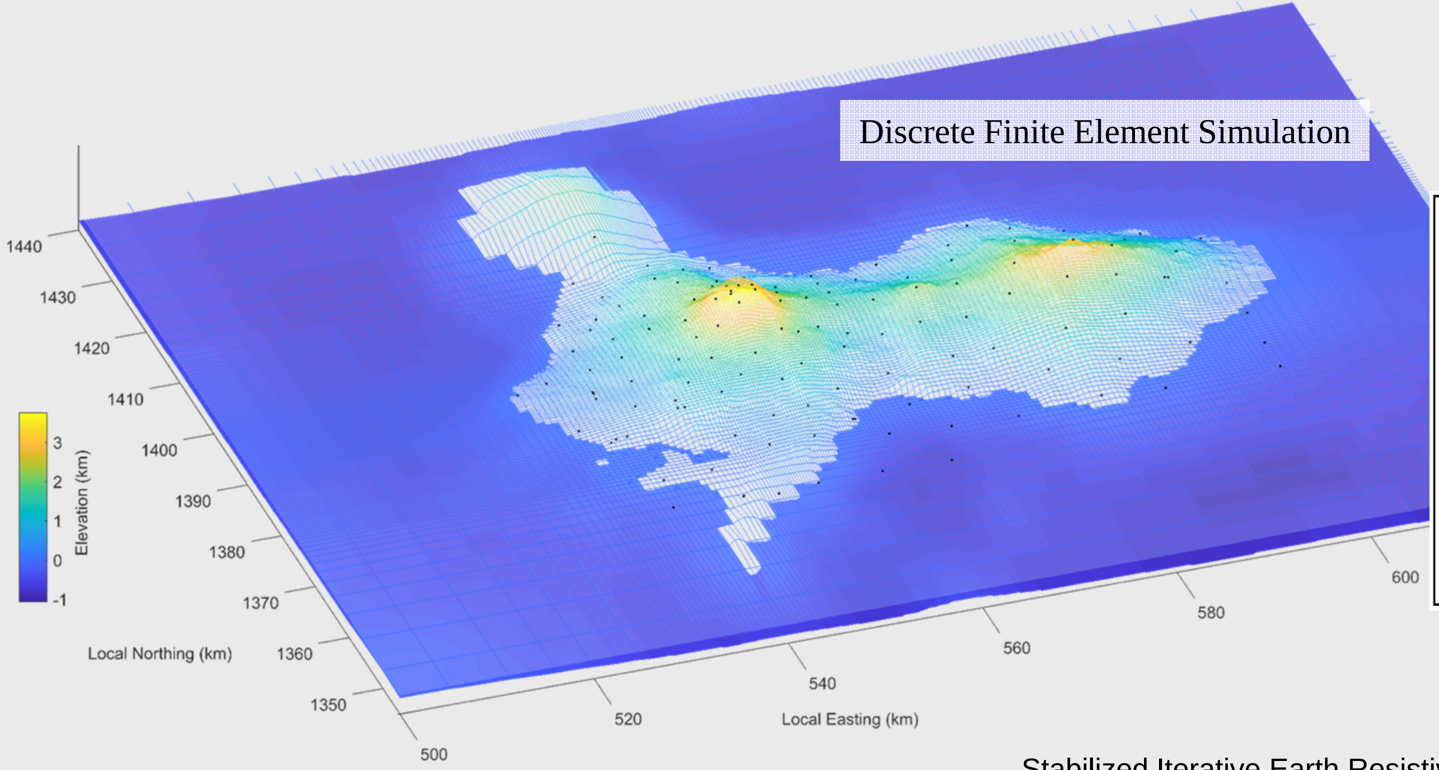

$$\nabla \times E = -i\omega\mu H \qquad \nabla \times H = \hat{\sigma} E$$

$$\nabla \times \frac{1}{\mu} \nabla \times E - i\omega\hat{\sigma} E = J^{imp}$$

$$E = \sum_{i=1}^{n_e} x_i N_i \qquad H = \frac{-\nabla \times E}{i\omega}$$

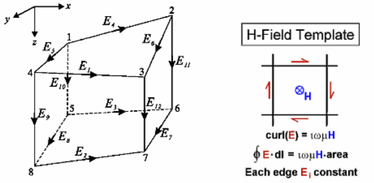

EM Field (Maxwell) Equations
And Deformed Finite Element

Objective: $W_{\lambda}(m) = \{(d - F[m])^T C_d^{-1}(d - F[m])\} + \lambda\{(m - m_o)^T C_m^{-1}(m - m_o)\}$

NL Step: $m_{k+1} - m_k = \{J_k^T C_d^{-1} J_k + \lambda C_m^{-1}\}^{-1}\{J_k^T C_d^{-1}(d_k - F[m_k]) - \lambda C_m^{-1}(m_k - m_o)\}$

Stabilized Iterative Earth Resistivity Voxel Estim. (Tarantola, 1987)
NL Step Recast to Data-Space Formulation (Parker, 1994)
Can Invert for Impedance Static Distortions (Avdeeva et al., 2015)
Direct Matrix Solutions Used Throughout (Metis, Pardiso, Plasma)
Parallelized on Large RAM, Single-Box Workstations

3D MT Inversion of Using Deformable Edge Finite Element Algorithm
(Kordy, Wannamaker, et al., 2016, GJI)

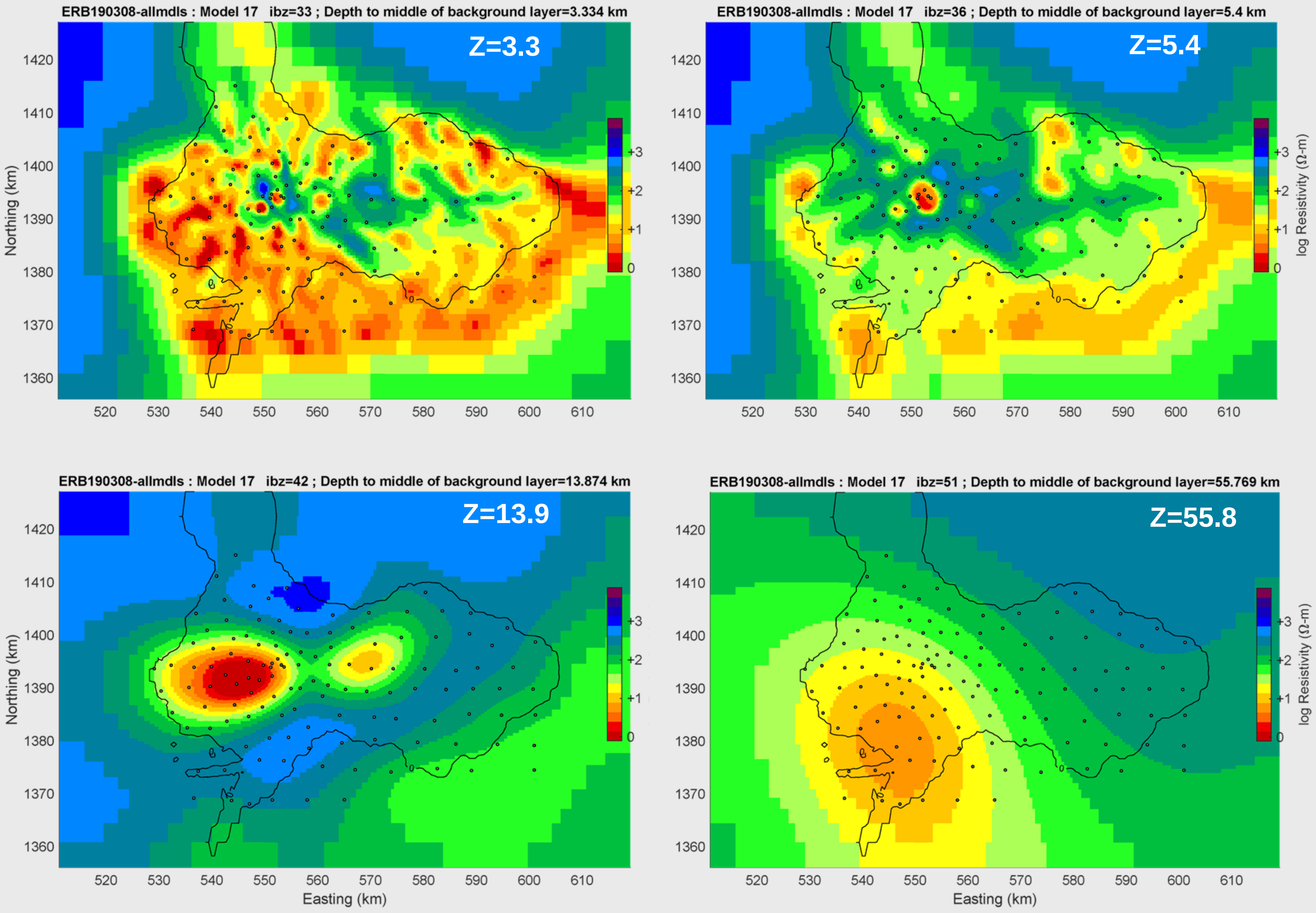

Mount Erebus MT Inversion Resistivity Plan Sections:

- General clay alteration blanket at shallow levels.

- Clear visibility of magmatic conduit and upper chamber by 5 km depth.

- migration of magmatic structure westward along apparent controlling E-W trend.

- Movement of magmatic plumbing southward from lower middle crust and deeper.

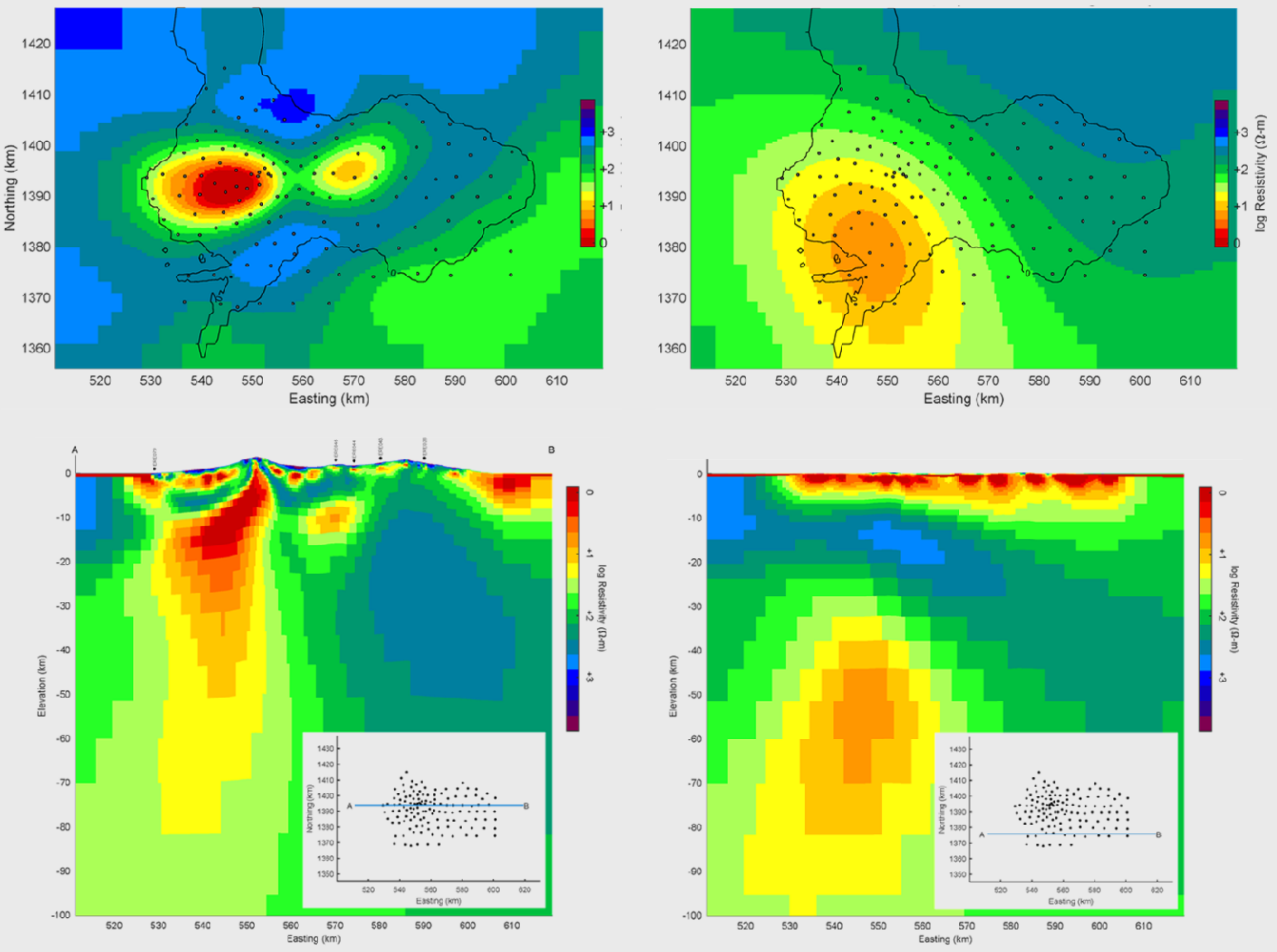

Mount Erebus MT Inversion Plan and Section Views

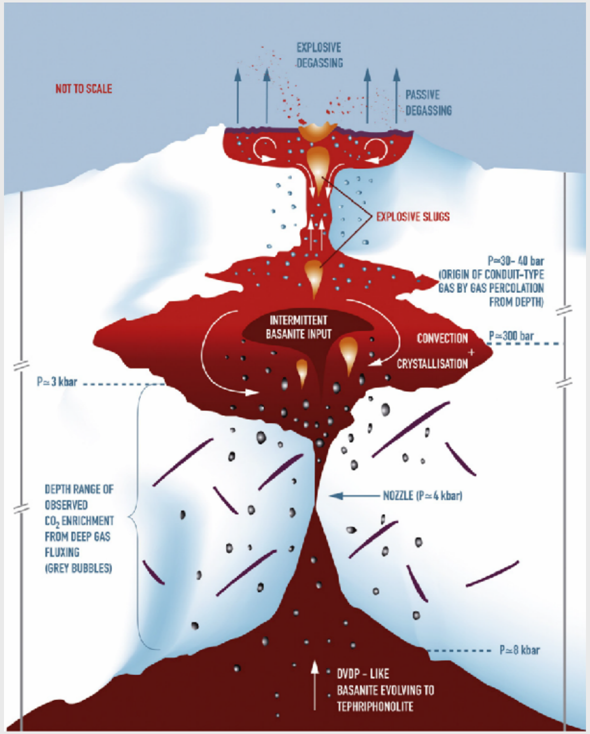

Schematic Mount Erebus magmatic plumbing (Oppenheimer et al., 2008). Note “Nozzle” interpreted at 4 kbar for periodic basanite replenishment.

Conclusions and Outlook:

- Key elements of MT method in t/s processing and in recognizing heterogeneity developed in 1970s & 80s
- 1990s saw methods for stable modeling of discontinuous E-field
- Current inversion algorithms capable of 1000+ sounding sets
- Proper understanding of petrological principles needed for consistent interpretation and to advance beyond “It’s fluids”
- External constraints on temperature most useful
- Active Great Basin extensional regime seems to exhibit “banana-split” model of crustal rheology
- Potential to evaluate geothermal resources for baseload power
- Wide-scale Juan de Fuca-Gorda hydration of upper mantle
- Carbonized horizons may assist resolving terrane assembly
- Encourage progress in understanding physico-chemical controls on earth material resistivity


The End!
MARSDEN FUND